Project Number: FJL- MQP - MARM

MODULAR ROBOTIC ARM

4/26/2015

Project Team/Authors

Derek Calzada-Mariaca *dmcalzadamariaca@wpi.edu*

Monica Preston *mjpreston@wpi.edu*

Yihao Zhou *yzhou2@wpi.edu*

Advisor

Prof. Fred Looft *fjlooft@wpi.edu*

Electrical and Computer Engineering
Systems Engineering

Table of Contents

Table of Figures

Acknowledgements

We would like to thank Fred Looft for his guidance through the system engineering approach to this project. We would also like to extend our gratitude to Mik Tan for his help machining, Joe St. Germain for 3D printing, William Appleyard for help machining and solving mechanical issues and Robert Boisse for ordering and advising.

Abstract

The following paper describes the process and results undertaken to create a modular robotic arm system. The intent of the project was to create a low cost modular robotic arms system with features seen in more expensive systems as such a product does not exist on the market today. By following a systems engineering approach, our team was able to develop a modular robotic joint in an attempt to fill this market gap.

1. Introduction

1.1 Problem statement

A modular robotic arm, which is both advanced and inexpensive, is not currently available on the market today. A consumer's choices consist of inexpensive but flimsy toy arms or commercial grade robotic systems with prices far above the affordability of the average hobbyist.

1.2 Goal Statement

The goal of our project was to design and build a controllable modular joint that could be used to assemble a robotic arm. The design and component selection for the joints would allow a relatively inexpensive arm to be assembled while still maintaining precision and accuracy in its movements. The objective was to fill the gap between the inexpensive but fragile toy arms and the strong, precise, but expensive industrial grade arms. The target users of the arm are expected to be hobbyists and students.

1.3 Objectives

In order to measure capstone project progress, certain objectives are needed. The objectives help guide the group as well as define the project early on. For the creation of a modular robotic arm, the following objectives were determined:

- Study robotic arm products currently on the market to determine gaps in features, pricing, and applications in order to determine the best market design goals (e.g. gap analysis).
- Specify Measures of Performance (MOPs), Measures of Effectiveness (MOEs) and Key Performance Parameters (KPPs) that will drive the design and design choices.
- Design prototype joints that are inexpensive but robust using proper engineering techniques.
- Perform appropriate trade studies to select system design components based on minimizing risks to achieve KPPs, MOEs, etc.
- Create a fully functioning joint prototype.
- Write software to demonstrate control the position and movement of the modular joint system and to be used for testing.
- Test the prototypes in various configurations and conditions to ensure that the design specifications are met.

1.5 Stakeholder Analysis

As part of a systems engineering approach, it was important to identify the stakeholders of the project. Each stakeholder or group of stakeholders was identified by an ID, a defined role, and their priority with regard to completing the project. The following stakeholders were determined:

ID	Stakeholder	Roll	Priority
SH 01	**Team Members**	D. Calzada, M. Preston, Y. Zhou - Engineering team designing and creating a modular robotic arm	1
SH 02	**Project Advisor**	F. Looft - Technology and overall advisor, grades, funding, equipment, and facilities	1
SH 03	**Customers**	End users of product - Determine market and need for features	2
SH 04	**WPI**	Co-owner, potential patent filing	2
SH 05	**Suppliers**	Various companies supplying parts (motors, chips, etc.) used in the robotic joints	2
SH 06	**Manufacturer**	Manufacturers of robotic joints if product is commercialized	3
SH 07	**OSHA**	Defines safety procedures used in design and manufacturing of joints	3

Table 1: Stakeholders

1.6 System Needs and Requirements

Certain system needs were decided upon for the arm in order to further define the capabilities of the end product. Needs were determined based on preliminary background research along with the input of our project advisor and other stakeholders. Each need was defined by an ID, a description, a reasoning behind the need, a link to the stakeholders who would be most concerned with the specific need, and a priority. Further, as appropriate a preliminary MOE/KPP was assigned to selected needs based on stakeholder input.

ID	Need	Description	Reasoning	Stakeholders	Priority
N 01	**Modular joints**	All joints should be able to be used in combination with any other joint(s)	Modularity allows a robot with an arbitrary number of degrees of freedom to be constructed based upon user needs	SH 01, SH 02, SH 03, SH 04	1
N 02	**Payload**	A joint should be able to lift a 1 kg load held at one meter horizontally from the axis of rotation	Without being able to manipulate a payload, a robotic arm would be nearly useless. Defining the payload also defines what applications the arm could be used for	SH 01, SH 02, SH 03	1
N 03	**Rotational velocity**	While under no load, each rotational joint should be able to rotate at at least 45 deg/s	This appears to be a reasonable speed which would allow tasks to be completed quickly enough	SH 01, SH 02, SH 03	2
N 04	**Rotational velocity under load**	A joint should be able to rotate at a minimum of 45 deg/s while holding a 1 kg load one meter horizontally from the axis of rotation	The robot needs to operate under load in a timely fashion	SH 01, SH 02, SH 03	2
N 05	**Motion constraints**	The joint should not interfere with the range of motion of other joints on the arm	If a joint is too wide, it could potentially interfere with the range of motion of the other joints	SH 01, SH 02, SH 03	2
N 06	**Length of joint**	Each fully extended joint should be approximately 15 - 20 cm long	The longer each joint is, the longer an arm will have to be to add joints and therefore degrees of freedom	SH 01, SH 02, SH 03	2
N 07	**Wire Safety**	The wires on the arm should present no safety hazard. Including, areas where fingers could be crushed	To meet safety standards	SH 01, SH 02, SH 03, SH 07	2
N 08	**Cost**	The price of materials for each joint should be no more than $150.	This is to keep the cost down for the end users as well as to fit in the market gap.	SH 01, SH 02, SH 03, SH 05, SH 06	1

Table 2: System needs

ID	Need	Description	Reasoning	Stakeholders	Priority
N 09	**Accuracy**	Any rotation to a software defined angular position should be within 1% of the full rotation of the joint	Allows arm to move to predictable positions through software commands	SH 01, SH 02, SH 03	1
N 10	**Precision**	Any three consecutive rotations to the same software defined angular position should be within 1% of the full rotation of the joint	Allows arm to repeat tasks in a predictable manner	SH 01, SH 02, SH 03	1
N 11	**Maximum weight**	Each joint should not weigh more than 0.5 kg	Motors towards the base of the arm will need to create enough torque to lift the rest of the arm. The lower the weight the lower the necessary torque is.	SH 01, SH 02, SH 03	1
N 12	**Range of motion**	A pitch joint should be able to rotate at least 120 degrees. A roll joint will be able to rotate at least 180 degrees	The range of motion defines the workspace as well as tasks that an arm may be able to perform with larger ranges of motion able to have larger workspaces	SH 01, SH 02, SH 03	2
N 13	**Power supply**	The joints should operate from a 12 VDC power source	All joints need to run off of the same voltage which in turn should be fairly a common voltage that sensors, motors and microcontrollers can use	SH 01, SH 02, SH 03	2
N 14	**On board electronics**	Each joint should contain a microcontroller and sensors needed to accept positional input and move to the desired position within the defined accuracy	Since it is a modular system, having each joint be at least semi-intelligent allows for easier setup and use	SH 01, SH 02, SH 03, SH 05	2

Table 3: System needs [con't]

1.7 Summary

Once all of the design needs were outlined, it was time to research current systems and available components and systems. This would allow us to draw inspiration from existing products as well as more accurately define the market gap in which our modular robotic was attempting to fill.

2. Background

2.1 Introduction

This section is a compilation of background research performed for this project. Background research includes a Gap Analysis of products already on the market, a study of possible materials to be used in manufacturing, and a study of various types of components (motors, power transmission, etc.) that were considered for use.

2.2 Gap Analysis

Before designing the modular robotic manipulator, the team first conducted a gap analysis evaluating existing modular robotic manipulators. The following is a detailed analysis of various products that have been used academically and commercially.

Low Cost Compliant Robotic Manipulator

The robotic manipulator shown in Figure 1 was designed and manufactured by Morgan Quigley, Alan Asbeck, and Andrew Ng with the Department of Computer Science at Stanford University [1]. The manipulator has seven degrees of freedom with a human-scale workspace. The maximum payload of the manipulator is 2 kg.

The key features for this manipulator are its zero backlash performance as well as being easily back drivable, which is one of the important features for human safety. In order for the arm to have the zero backlash, a stepper motor together with a timing belt and a cable driver are used. In order to allow the robotic manipulator to safely interact with humans, it uses a series elastic design and reduces the flying mass to less than 4 kg by keeping the motors close to the base.

The robot used a stepper motor because it provides a large torque at low speed. Stepper motors also act as an electromagnetic clutch; therefore in the event of power loss, it can remain stationary while conventional motor may continue rotating. A disadvantage of using a stepper motor is if the motor slips, the arm position is unknown. Another reason of using stepper motor is a high performance DC brushed motors cost much more than the stepper motor with the same performance level. The robot manipulator uses joint encoders to achieve closed-loop PID control.

The force sensing was accomplished by measuring the displacement of the series elastic component, which will be discussed later. The overall structure was made of plywood in order to minimize weight and a laser cutting machine was used to manufacture all the components. The group used OROCOS-KDL kinematics library in C++ to control the motion of the arm and integrated the software with ROS to graphically simulate the arm on a computer.

The obvious disadvantage of this arm is that using series elastic actuators with cables makes the arm difficult to build. To assemble such arm requires expert skill, which is not our intended customer base. The structure material was plywood and all the motors are exposed without protection this make the arm brittle and a potential safety risk to users.

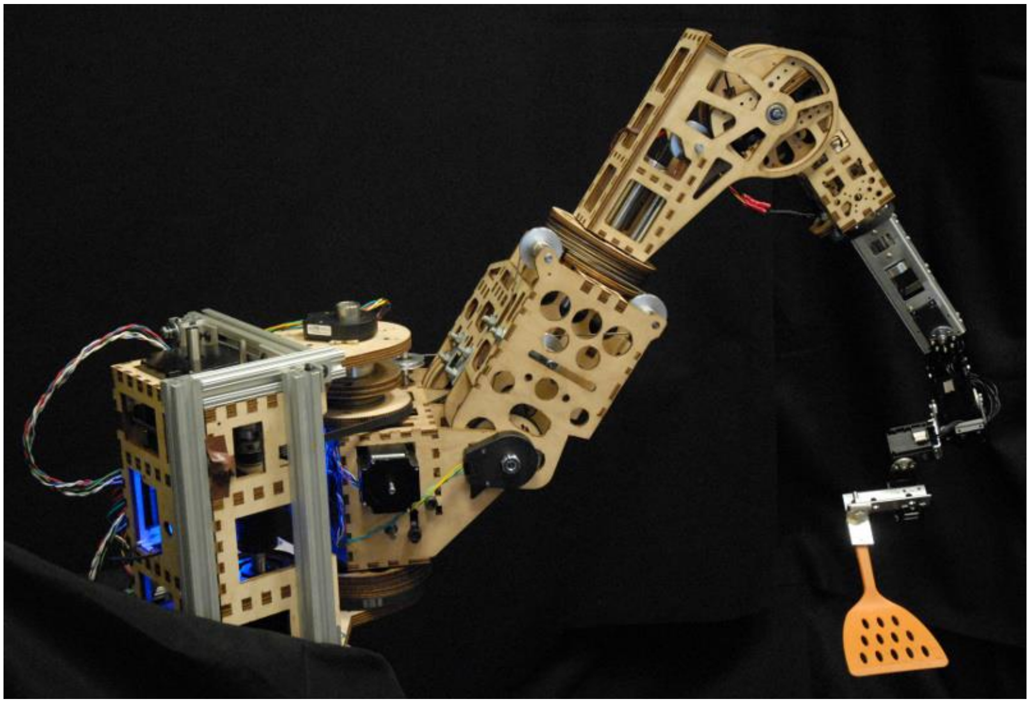

Figure 1: Low cost compliant robotic manipulator [1]

Low Cost Robotic Manipulator Joint

A similar project to the one that we are tasked with was worked on in 2009 by capstone project students [2]. Their goal was to design and build a modular robotic manipulator joints that were low cost and highly accurate. There were two different types of joints, an elbow joint and a rotator joint. In the design phase, they had three iterations for both joints. In their design, each joint is able to receive data and electrical power, generate motion, and transfer data to the next joint. As shown in Figure 2, one of the designs for the elbow joint used a worm gear drive system, which prevents backlash while providing a high static torque. The disadvantage of a worm gear is if the robot arm were to experience high external force, it may damage the gears. This version was never implemented or tested by the 2009 team.

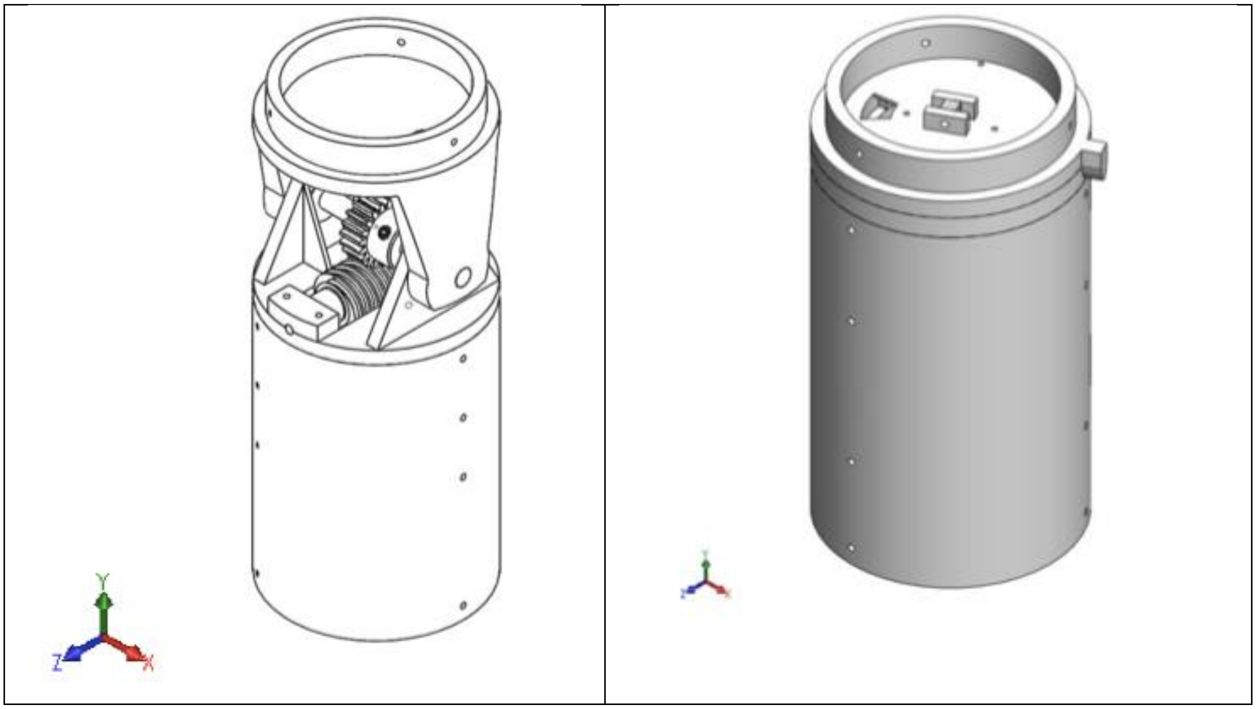

Figure 2: Low Cost Robotic Manipulator Joint [2]

SCHUNK Powerball Lightweight ARM LWA 4P

The industrial robotic arm joint show in Figure 3 was design by SCHUNK Inc. A multinational manufacturing company based in Germany [3]. The Powerball controls the rotation of two axes, oriented 90 degrees from each other. This allows the single joint to have 2 degrees of freedom and to perform both pitch and rotational motion. The combination of three Powerballs results in 6 degrees of freedom allowing the arm to reach any point in a workspace.

The Powerball has universal CANopen communication interfaces and cable technology that was designed by SCHUNK for data transfer, power supply, and as a way to easily integrate with other modules. The joint module uses brushless DC motors with permanent magnet brakes. Compared to other industrial arms, the Powerball is more compact and has better mobility and quick-change system. The battery allows for an 8-hour operation time without charging. However, the high cost of the arm limits the customers to large factories.

Figure 3: SCHUNK Powerball Lightweight ARM LWA 4P [3]

igus Robolink

The igus Robolink shown in Figure 4 is a five degrees of freedom serial manipulator driven by cables. It was designed and manufactured by igus, a German based worldwide manufacturer and distributor of different types of plastic products [4]. The manipulator joint is made of fine polyamide and carbon fiber. The cables, which control the joints, are made of Dyneema, a high-strength synthetic fiber that has a tensile strength of 4,000N. The links between joints are made of aluminum tube. This results in a relatively light weight arm. In order to largely reduce the moving mass, the actuators and control module are separated from the body of the manipulator. Because motors are not directly mounted on the manipulator, the weight of the motor does not create a moment force on the arm. Stepper motors are usually the first choice with their system. The Robolink manipulator has four different joints, a rotating joint, a pivoting joint, a base joint, and a 2-axis joint.

Figure 4: igus Robolink [4]

Users can assemble this arm with different combinations as seen in Figure 5. A few advantages of the Robolink arm are that they are lightweight, compact, flexible, modular, compliant, and waterproof. The Robolink can be controlled by any control solution, such as PLC, SPC, Matlab, ROS etc. The cost of the Robolink is about $370 - 750 per joint without the motor, and one six degrees of freedom arm with complete actuating system costs about $6000. This price point is low-cost when compared to the Powerball but is likely out of the budget of a hobbyist. Another disadvantage for the Robolink is that although each joint is modular and lightweight, the heavy motor box still prevents the arm from being portable. Besides this, assembly takes time as each cable must be run from the motor, throughout the arm until it reaches its respective joint.

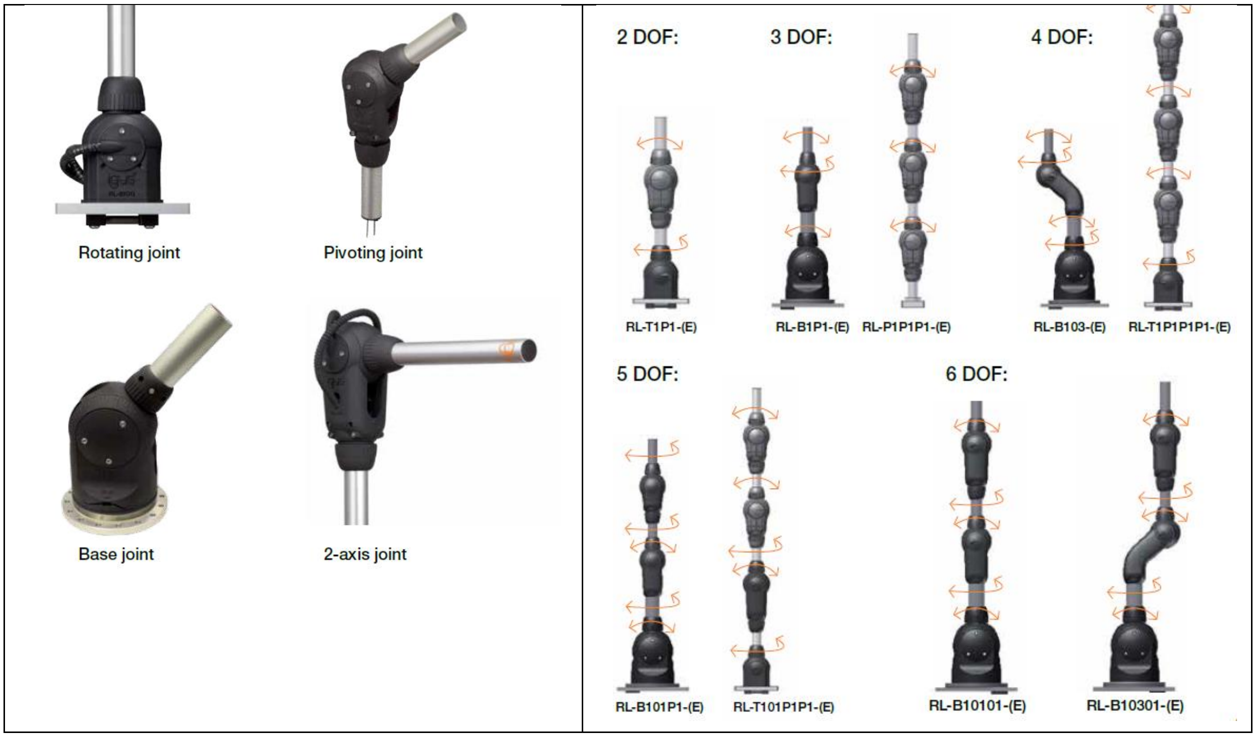

Figure 5: Various joints and possible configurations of the igus Robolink [4]

Kinova Jaco Robotic Manipulator

The Jaco robotic manipulator was produced by Kinova, a Canadian company engaged in the design and manufacturing of innovative personal robotic products [5]. The Jaco robotic arm is the size of human arm. It was designed for rehabilitation and can be mounted on any assistive equipment such as a wheelchair. The manipulator has six degrees of freedom and can reach the distance of 0.9m. The body is made out of carbon fiber, which results in the arm weighing 5.7kg. A DC brushless motor combined with a 1:100 gear ratio Harmonic Drive allows for a maximum payload of 1.5kg. The arm has a powerful control system with a 1 Mb/s CANBUS to provide fast data transfer between each joint. The arm can be controlled using any existing controlling software. Kinova also provides control software as well as an API. The retail price of Jaco manipulator is about $48,000 making it much too expensive for a student or hobbyist.

Figure 6: Kinova Jaco Robotic Manipulator [5]

Table 4 below compares these arms.

	Low-cost Compliant Robotic Manipulator	Low-cost robotic manipulator joint (MQP)	SCHUNK Powerball Lightweight Arm LWA 4P	igus Robolink
Degree of Freedom	7 DOF	1 DOF per joint	2 DOF per joint	1-DOF Rotating Joint, 2-DOF Swiveling and rotating joint
Maximum Payload	2 kg (4.4 lb)	1000g for rotator-joint, 500g for elevator-joint	6 kg	pivoting: 1.2kg, rotation: 0.5kg, 6-DOF link: 0.5kg
Size	Length 1.0 m to the wrist		grip radius > 700 mm	Link 1: 285.75mm Link 2: 450.85mm Link 3: 450.85mm
Repeatability Accuracy	<= 3mm	unknown	0.06 mm	1-2mm
Drive	Low-cost stepper motors with timing belt and cable drives and the series-elastic components	ML-50 50:1 Permanent Magnet Geared Motor, Beetle B231 Gear motor 231:1	Brushless DC Motors with permanent magnet brakes, harmonic drive gear	5 EC 45 flat Ø42.8 mm, brushless, 50 Watt, with Hall sensors.
Dead Weight	11.4 kg (25 lb)		12.5 kg	345g
Joint Speed	1.5 m/s		72°/s under nominal load	5-10 cycles/min
Power Supply	12V DC	12V DC	24V DC, 3A avg., 12A max	24V DC / 10 A
Cost	$4,135	$291.68 for elevator-joint, $203.04 for rotator-joint		Approximately $6000 for 6-DOF arm, $370 - 750 per joint without motor
Communication	RS485		Universal CANopen communication interfaces	
Range of motion			±170°	Pivot: ±90°, Rotation: ±170°
Control System	ROS with OROCOS-KDL Library		ROS node or KEBA CP 242/A	Compatible with any control solution
Material	Plywood	Plastic	Metal	Plastic & Aluminum

Table 4: Comparison of robotic arms

2.3 Material Study

When designing and manufacturing our robotic joint, there were a wide range of metals, plastics, and composites from which the joint could be produced. Each of these materials has its own advantages as well as disadvantages. In order to determine which would be suitable for this application, the various options were studied. In Table 5 below, popular mechanical design materials are compared.

	Young's Modulus (GPa)	Tensile Yield Strength (MPa)	Ultimate Tensile Strength (MPa)
Aluminum 6061	276		310
Steel (SAE 1040 hot rolled)	207	290	524
Brass	110		250
PVC Pipe	2.3	51	
PLA Plastic	3.5		50

Table 5: Material Properties

In addition to considering the physical properties of each material, their ease of manufacture is another important design consideration. PLA plastic, used commonly in 3D printers, is very easy to work with and can be formed into complex designs quickly. The downside being a PLA part is not as strong as an equivalent mental piece. For this reason, a 3D printed part would be ideal for a prototype or non-loadbearing part. Even within metals, the manufacturing advantage is something to be considered. As seen in Table 5, steel has a much higher tensile strength than Aluminum but when machining, aluminum is a much easier material to work with.

2.4 Components Study

Motors

Motors are the most important component in the robotic arm system. There are two classes of motors: alternating current (AC) motors and direct current (DC) motors. The power of motors can range from 1/100 hp to 100,000 hp and the rotation speed can range from less than 0.001 rpm to 100,000 rpm [6]. The physical size of motors also varies in a large range. Because our robotic arm requires modularity, meaning that the system is powered by external battery, we limited the selection to DC motors. The diagram below lists most of the existing DC motors.

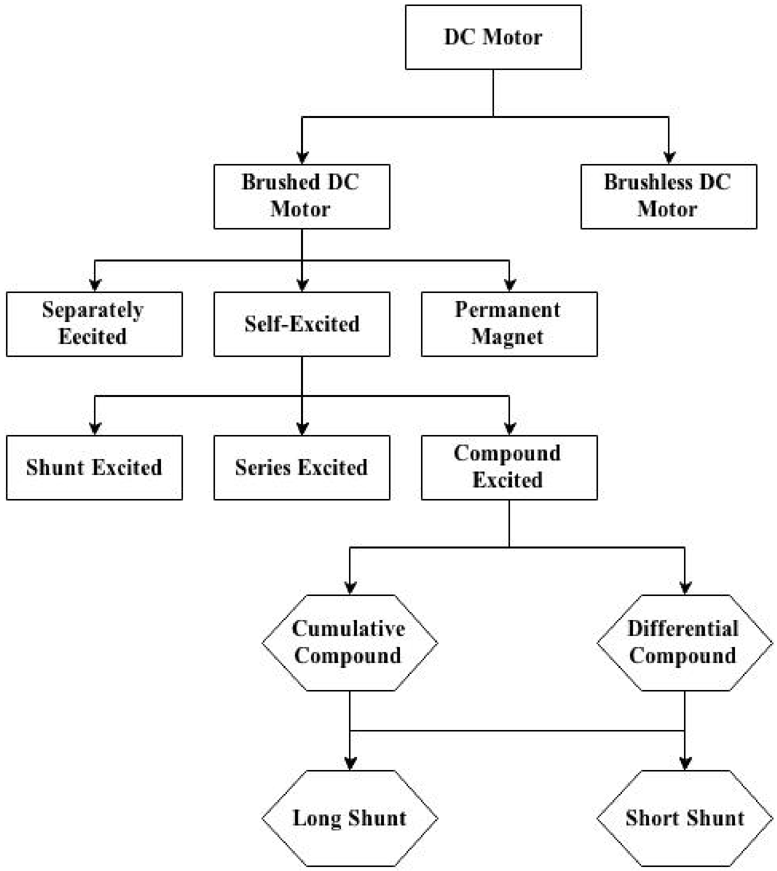

Figure 7: Types of Motors [6] [7]

There are three main types of DC motors: stepper motors, brushed DC motors and brushless DC motors. The brushed DC motor is an internally commutated electric motor that has been used for over 100 years [8].

The four essential parts of a brushed motor are the field winding, armature winding, brushes, and commutator as seen in Figure 8.

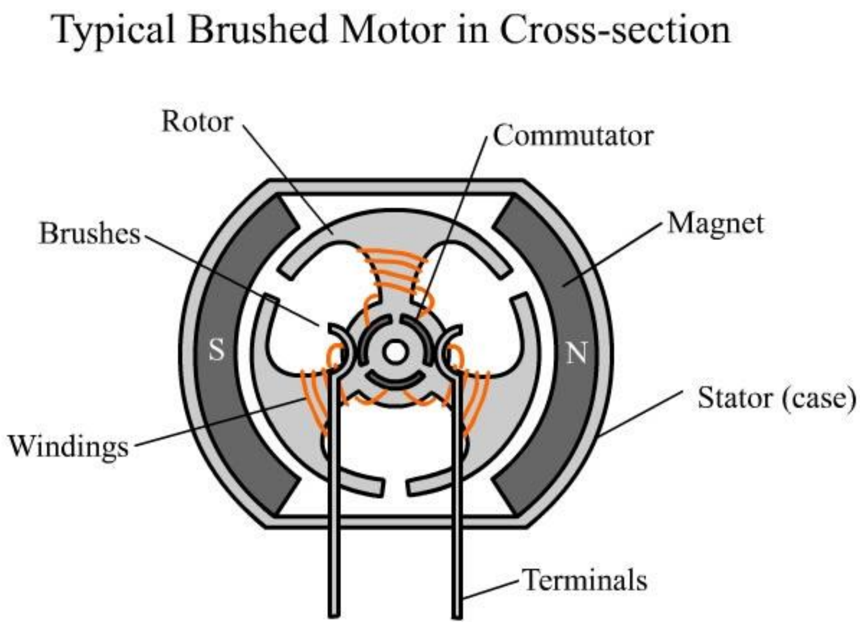

Figure 8: Illustration of a brushed DC motor's components [28]

The field winding is used to generate the magnetic field if a permanent magnet is not used. Once current is applied, a magnetic field is generated around the armature which pushes against the magnetic field generated by the field winding. The magnetic force then drives the armature to rotate. The brushes of the motor are made with graphite material, making contact with the commutator and transferring the current from commutator to armature. When the armature winding becomes horizontally aligned with the field winding, the magnetic field generates zero force. At this point, the commutator reverses the direction of current, reversing the magnetic field [8].

The brushless motor was first used in 1962. It overcomes many disadvantages the brushed motor has. A brushless motor replaced brush and commutator with an electronic controller to continually switch the phase to the winding to keep the motor rotating. Instead of rotating the armature, a brushless motor rotates the permanent magnets around a fixed armature [9].

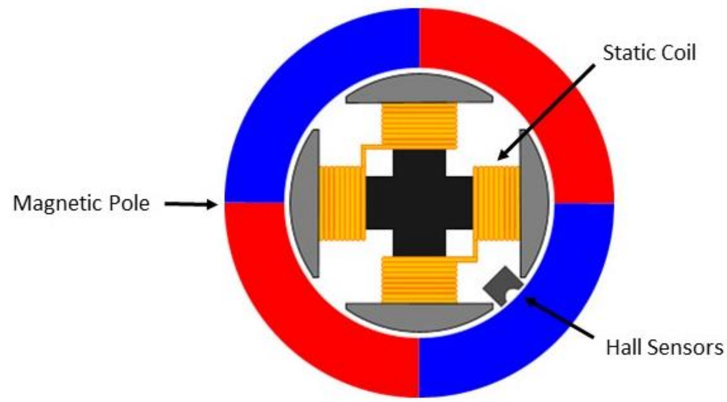

Figure 9: Illustration of a brushless DC motor's components [17]

A typical brushless motor uses Hall sensors (shown as a grey square with a semicircle cut-out in Figure 9) to detect the change of the magnetic pole and switch the coil (seen as yellow lines in Figure 9) on and off accordingly. It works similar to the brush and commutator on brushed motor. In a brushless DC motor, the permanent magnet, which alternate in polarity (shown as the blue and red ring), rotate around the static coil core as the coil's polarity is quickly alternated between two polarities.

A stepper motor is a special type of brushless DC motor that divides a full rotation into many steps (shown in Figure 10). Each step has equal angle and the motor can be commanded to move and stay at one of these steps [10].

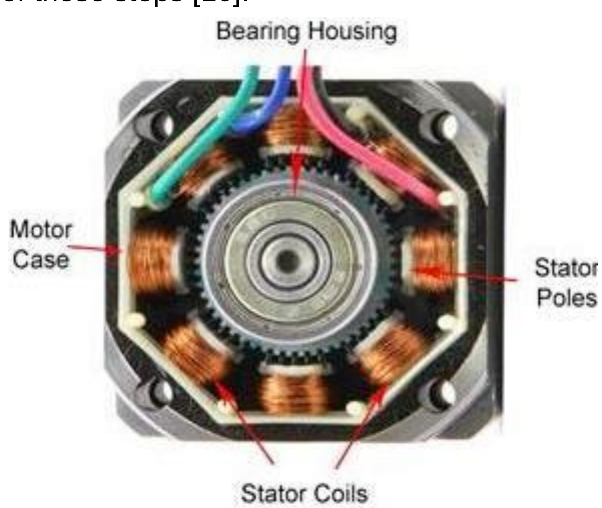

Figure 10: Illustration of a Stepper motor's components [18]

Compared to regular brushless DC motor which usually works together with a feedback encoder, a stepper motor has better motion control because it is operated in steps. As long as the motor does not skip steps, accurate position control can be achieved in an open loop system. However, if the motor skips steps, the motor position needs to be recalibrated. Adding an encoder to the shaft can solve this problem. A stepper motor also has a large holding torque because the winding current flows through the motor even when the motor stops moving. However, it wastes a lot of energy by holding the torque at the position.

In order to making a proper decision in terms of the motor type the team will be used for the project, the comparison table has been made. The table below lists all the advantages and disadvantages of brushed motor, brushless motor and stepper motor.

	Brushed Motor	**Brushless Motor**	**Stepper Motor**
Pros	● Low cost ● Simple control ● No controller is required for fixed speeds ● Can operate in extreme environment	● Electronic controls the motor ● No sparking and less noise ● No need to replace brushes periodically ● Easy to cool down ● High efficiency ● Higher speed range	● Electronic controls the motor ● No sparking and less noise ● No need to replace brushes periodically ● Easy to cool down ● Higher speed range ● Accurate motion control ● Maximize holding torque
Cons	● Needs to replace brush periodically ● The brush causes friction and reduces the torque ● Poor heat dissipation ● Higher rotor inertia ● Lower speed range ● Brush generates noise and sparking	● Higher cost ● Complex control ● Requires an microcontroller to run the motor	● Higher cost ● Requires an microcontroller to run the motor ● Energy inefficient ● Needs to recalibrate if motor skip steps

Table 6: Comparison of DC electric motor types [11]

Power Transmission

Harmonic Drive Gear

A Harmonic Drive Gear, also called a strain wave gear, is a type of mechanical gear system based on elastic dynamics. According to the definition from Oxford Dictionary, harmonic drive is a reversible reduction drive providing a large reduction ratio with effectively zero backlash, high torque capability, and high efficiency [13]. The drive has concentric input and output shafts and is of considerably lower mass and volume than comparable drives.

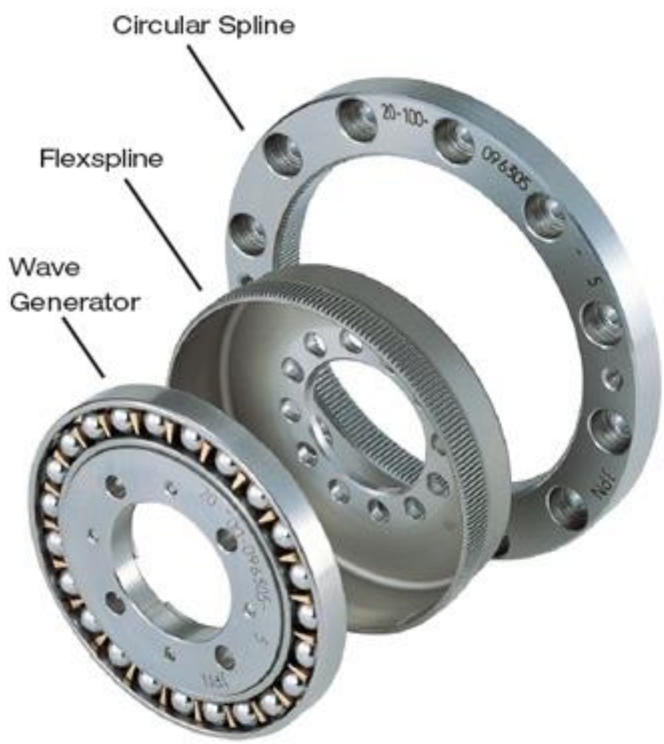

Figure 11: Harmonic Drive Gear [12]

As shown in Figure 11 above, the mechanical system consists of three basic components: wave generator, which is an elliptical disk contains outer ball bearings; flexspline, which made of an elastic material (usually a thin walled steel cylindrical cup); and the circular spline, which is a rigid circular ring with teeth on the inside edge. The harmonic drive works by directly connecting the motor shaft to the wave generator. As the motor drives the wave generator rotating, the flexspline teeth, which are meshed with those of the circular spline, change [12].

The flexspline has fewer teeth than the circular spline has; therefore for every full rotation of the wave generator, the flexspline rotates only a little, which reduces the output speed. The reduction ratio can be calculated as formula shown below:

$$Reduction\ ratio\ =\ (flex\ spline\ teeth\ -\ circular\ spline\ teeth)\ /\ flex\ spline\ teeth$$

A harmonic drive has many advantages comparing to other gearing mechanism. Including: simple structure (3 components), compactness, light weight, zero backlash, achieving high gear ratios with less space, high positional accuracy, high repeatability, high torque to weight ratio, coaxial input and output shafts, and constant performance without wearing [12]. Due to the many advantages harmonic drive systems have, they have been largely used in areas including: industrial machine, robotics, aerospace, medical equipment, and radar tracking systems etc. Harmonic drives have many different types in accordance with different requirements. The criteria of selecting the proper drive type includes input/output torque ratio, lubrication type, output rpm, size and weight, maximum backlash, and maximum transmission error [14].

Series Elastic Actuator

Series elastic actuators are an unconventional design of robotic arms and legs. The idea is to introduce the elastic component between motor and load, mimicking the structure of human muscle. The traditional design between motor and load was to use a gear train to reduce the speed. However, using gears causes friction, backlash, torque ripple, and noise. To solve some of the problems listed above, a compliant component is added between gear train and load, as shown in Figure 12 below.

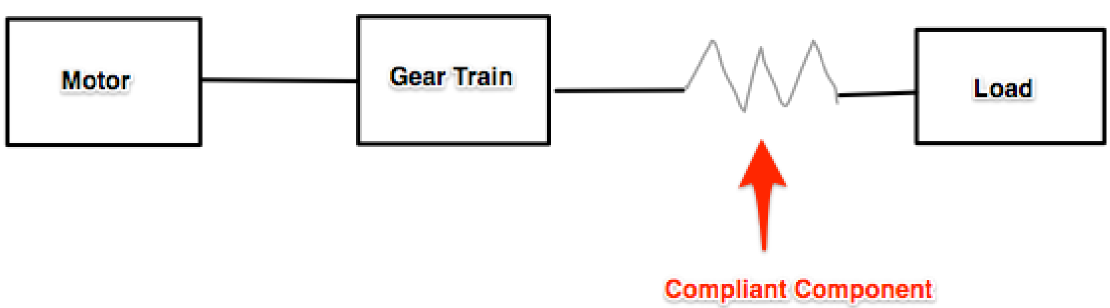

Figure 12: Diagram showing setup of a series elastic actuator

There are many advantages of using a series elastic actuator as well as disadvantages as shown in Table 7.

Advantages	Disadvantages
Human safety and less chance to damage the environment	Less precision
Accurate and stable force control	Takes more space
Shock tolerance	Not as stiff
Lower reflected inertia	Complex design
Energy storage	

Table 7: Advantages vs disadvantages of a series elastic actuator [15]

One remarkable advantage of a series elastic actuator is it allows the robot arm to have more accurate and stable force sensing than any other force sensing method such as a strain gauge or a current sensor. By calculating the difference of displacement between motor and load, multiplied by the elastic coefficient of the compliant component, we know how much force is exerted to the load. Figure 13 below is one example of applying series elastic actuator to the robot. This is the robotic leg that was made by a WPI graduate student as his research project. Series elastic actuators are used for all the joints the robot has.

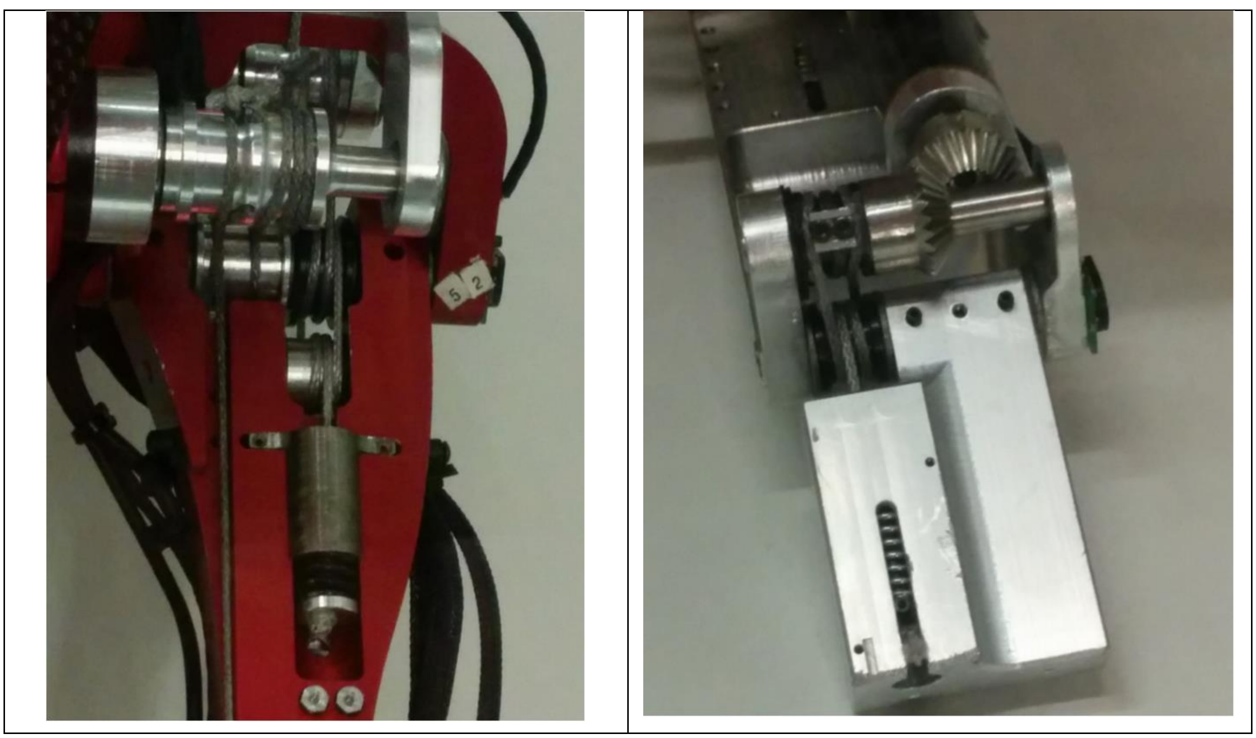

Figure 13: Series elastic actuator used in a WPI project [16]

3. Methods

3.1 Introduction

In order to ensure that the task specifications devised in earlier portions of the projects were met, certain methodologies had to be followed. Those selected can be seen below alongside with reasoning behind selecting each.

3.2 Methods

From the beginning of the project, a systems engineering approach was used. Background research was conducted to understand the market gap and create a project proposal. A market gap was identified and certain design specifications and goals were chosen. This technique was decided upon to run the project as it would be ran in an engineering company.

Figure 14 below is the "V" of systems engineering [29]. On the left side of the V the project is decomposed to know the finer details and make a concept design. The system requirements for our project are our design specifications. In the initial design section our high level design is outlined.

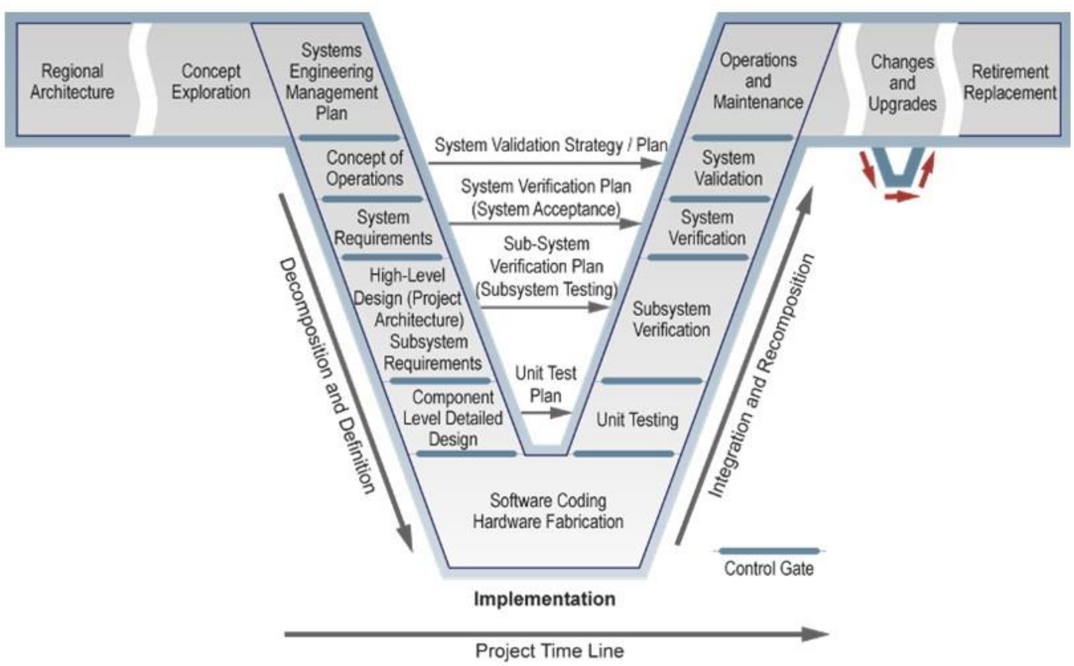

Figure 14: The Systems Engineering Approach [29]

After research was completed, various designs were considered. This was in an attempt to find a broad number of solutions to the problem outlined in the project. Each design was ranked via various weighted criterion such as cost, ease of manufacturing, precision, etc. There were multiple charts made to understand all options. Each of these focused on a different design idea including drive trains and degrees of freedom, Figure 15. The highest ranking design aspects were then selected and combined as the base design to further develop.

	weight %	1DOF rotation varying configuration	2DOF pitch and rotation	1 DOF ROT/1DOF Pitch
Cost	30	3	2	2
Modular joints	20	3	2	1
Minimum payload	10	2	2	2
Length of joint	15	3	1	2
On board electronics	5	2	3	2
Weight of joint	20	3	1	3
		2.89	1.7	2

Drive train		Only Linear	Worm	Series Elastic with Worm	Series Elastic without Worm
Cost	20	3	2	1	1
Not back drive able	20	1	3	2	1
Accuracy/ back lash	20	2	3	2	1
Speed	20	3	2	2	3
Size	20	3	3	1	1
		12	13	8	7

Figure 15: Design Charts

Once a general design was selected, modeling of the parts was started. SolidWorks was used as the primary design and simulation program for the physical models of the joints. Parts were created and assembled in order to test the viability of each design. Aspects such as motion and stress can be simulated without needing to create a physical prototype. This saved both time and money adding to the efficiency of the design process.

Concurrent with the mechanical design, the electrical components were also selected and designed. Because of the desired level of control and intelligence within each joint, wiring diagrams and custom circuits had to be mapped out digitally before being prototyped to ensure that they would work as desired.

After completion of a test circuit, programming could be started. Using a software engineering approach, various features were first selected. From there, the simplest of the features were instituted and tested before progressing to a more complex, full program

Once the digital version of the prototype is tested, a physical one was built. The prototype was made of readily available materials. After the creation each of the prototypes, physical testing was done to ensure that the design specifications were met.

3.3 Summary

After the methods of completing the project were decided upon, the process of implementing these systems began. This began with creating a design based off our system needs using the systems engineering approach.

4. System Design

4.1 Mechanical Design

Explanation of mechanical design

The first section of the joint that was designed was the gear system. It was believed that this would be the most important design factor in determining the physical size of the joint and would therefore determine how the rest of the physical system was configured. After the most compact possible gearing solution was determined, the body was designed to fit as tightly as possible around it. A circle was drawn with its center in the axis of rotation of the output whose radius extended to encompass the gears. The result was a 4.25” diameter circle which would form the base of the cylinder-like shape of the joint. Because of the geometry of the worm and worm gear, the distribution of the gears within the body of the joint ended up being lopsided as seen in Figure 16. This allowed for wiring and electronics to be placed within the empty side of the body.

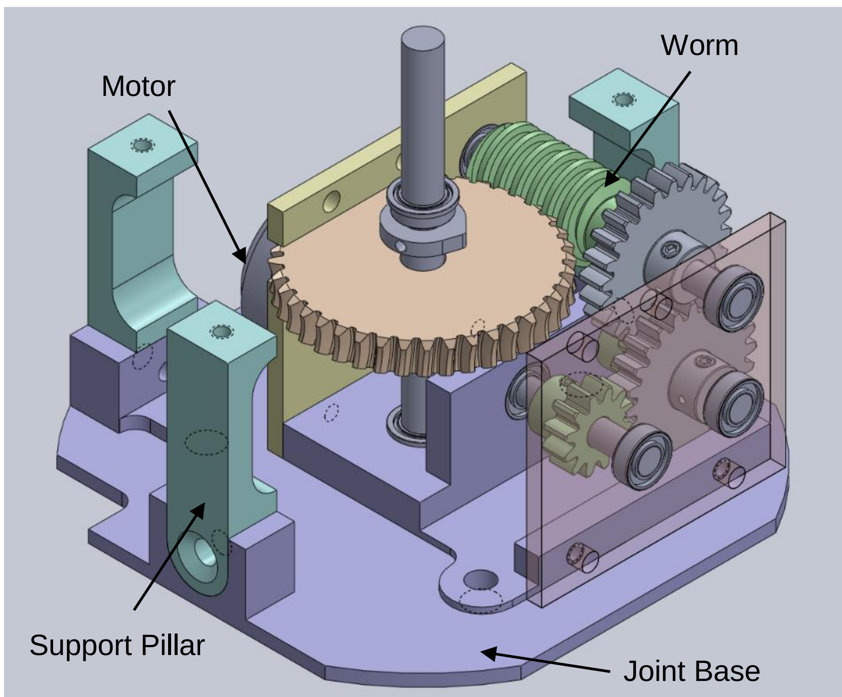

Figure 16: Internal gear configuration

The final gear ratio achieved in our design was 160:1 with 160 revolutions of the motor shaft resulting in one full revolution of the output shaft though this was in reality limited to 270°. In order to achieve the 160:1 gear ratio, three gear reductions were used, two being with spur gears and the last with a worm and worm gear. A worm gear was used because they allow high torque to be generated as well as prevent back driving of the output shaft. This meant that our joint would be both strong enough to meet our design specifications as well as that power would not have to be provided for the joint to retain its static position. The tradeoff with this type of gear is that its efficiency can range from 90% down to 50%. The spur gears used consisted of two 12 tooth and two 25 tooth gears. This meant two 2:1 gear reductions. The benefit of spur gears is that they have a relatively high efficiency of 94-98%. In our case, the disadvantage was that in order to achieve a high enough gear reduction, the output gear would be four times larger than the input gear for the 4:1 reduction needed. Since the gear system would have the greatest influence on overall size of the joint, two 2:1 reductions were used in order to be more compact.

Initially this project was envisioned as having two different types of joint, one for rotation along the arm axis and another for rotation offset 90° from the arm axis. This idea was eventually dismissed in favor of using one joint to achieve both types of rotation. As seen in Figure 17, by using a joint which was at its core is two cylinders stacked on top of each other which could rotate in line with each other, along with linkage adapters, a joint could be created which would fulfil the roles of both aforementioned joints.

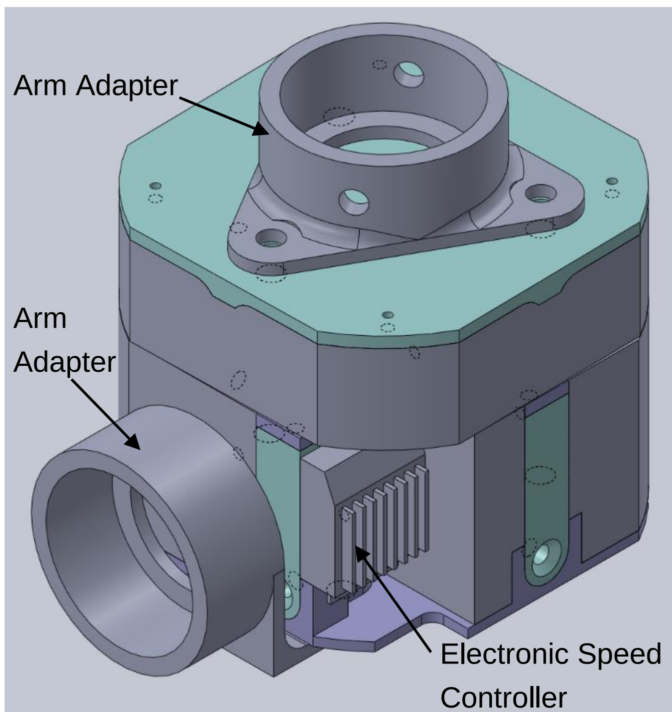

Figure 17: Picture of both types of linkage adapters

By the end of the design phase, there were two different versions of the robotic joint designed. The first one was nearly completed before the second one was started. This second version was created due to several problems in the original design, key amongst them were manufacturability and strength. Though this was a new design, many ideas used in the original were used.

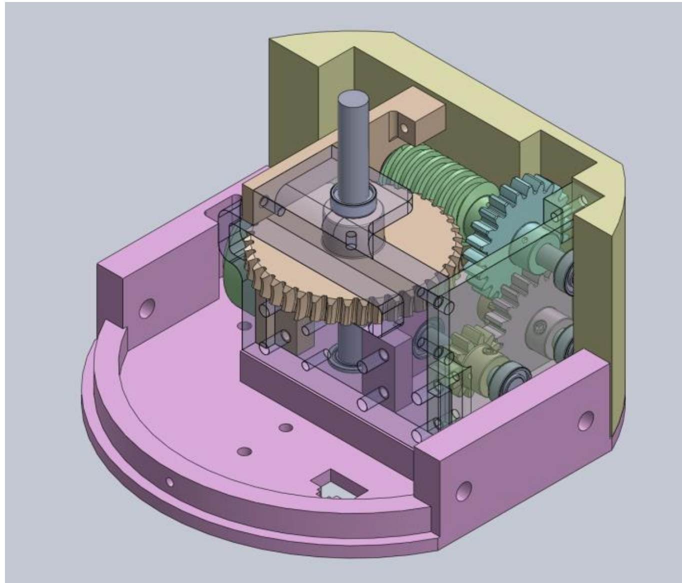
Figure 18: First version of the joint design

Between the two designs, the same gear arrangement was used although in the new version, the metal plates which hold the bearings are no longer as critical to the strength of the body. This was due to the introduction of three support pillars. In the preliminary (or first) design, most of the shear stress on the shaft would have been transmitted through a plate on the side of the joint with the rest being supported by the plates holding the bearings of the gear system. These new pillars added rigidity to the body of the joint while also distributing any stress more evenly.

During initial brainstorming, the wires which supplied power and serial communication would have entered through plugs on the bottom of the joint and exited through the top. It was later realized that this may cause wires to become tangled around internally as they would have to rotate between the two halves. For this reason, the final version has all wiring and electrical components in the bottom half of the joint. The circuit board was designed such that the top of the joint could rotate around the bottom without interfering or snagging on any wires.

In order to save weight, the structural components of the joint were machined out of aluminum while the outer shell was 3D printed. Since PLA plastic is less dense than aluminum, weight was saved while still being able to contain all the internal components of the joint within a shell.

FEA Simulation

The CAD model was tested using the simulation package in SolidWorks. Screws were added to the analysis to achieve the most accurate result. A force of 1N was applied to identify the critical points in the model. There are many orientations that the joint could be placed in the arm. The test run had the bottom fixed and a rotational torque about the center shaft. This would be if the joint was orientated as a rotary joint. Figure 19 displays the results of the deflection test. The largest deflection was on an arm of the top cross with a value of 3×10^{-4} in.

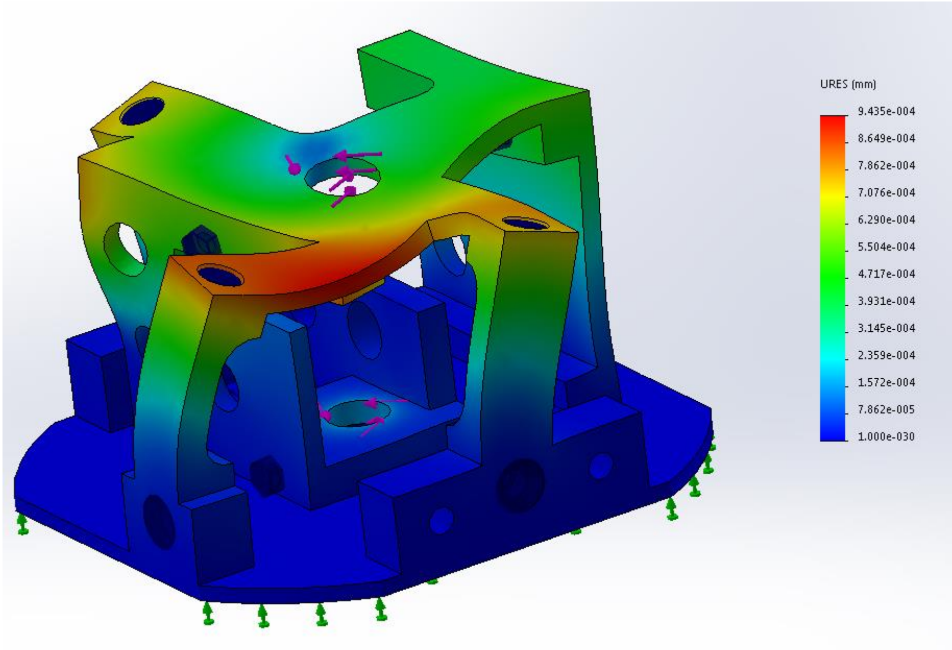

Figure 19: Deformation Result

In Figure 20 Von Mises stresses are displayed on the part with the same input conditions as the deflection analysis. As expected the highest stress of 3×10^6 N/m^2 is at the surface of force application.

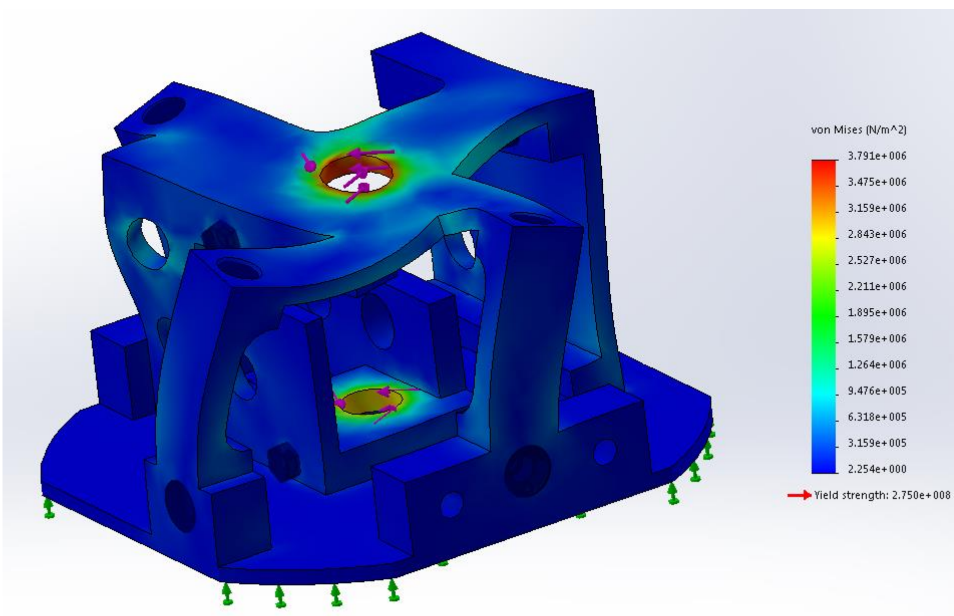

Figure 20: Von Mises Stresses

Machining

First, a 3D printed model was printed and assembled to verify fits of gears and electronic components. In Figure 21 the model is show without the bearing plates to allow the inner features to be seen.

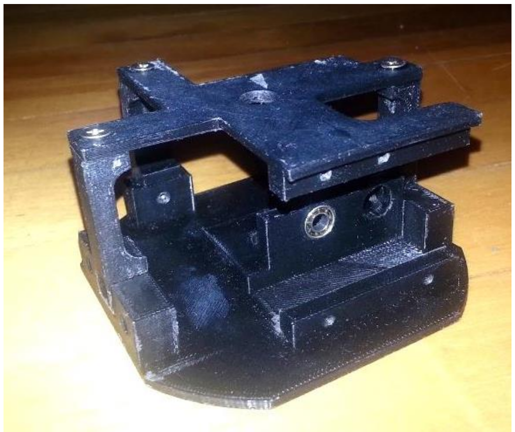

Figure 21: 3D printed prototype

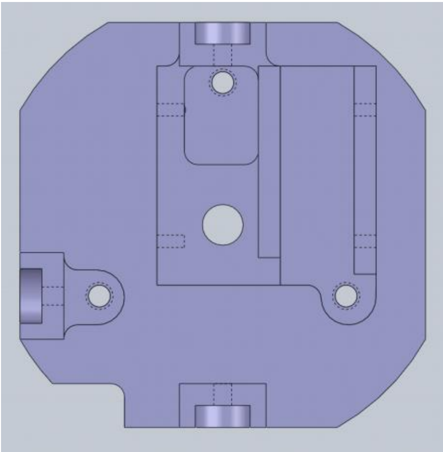

Figure 22: Rounded edges can be seen in all the inside corners of the base

Rounds were added to the inner features of the parts to allow for manufacturability as seein in Figure 22. Below is a diagram of the manufacturing process. From the SolidWorks model, G code is generated using Esprit, a CAM software. To prep the machine, tools are assembled, the tools and parts are probed, and the stock is fixtured. The Haas MiniMill, VM-2, and Drill Mill Center were used to create all the parts.

Figure 23 shows a screenshot of Esprit to make the vertical support. To use Esprit first chains are made that reference the main geometry. These chains are in the program manager on the left and are shown in blue in the graphics screen. Milling operations reference these chains for the tool pat. To make the vertical support the contouring of the part was done with a ⅜” endmill. A ½” ball end mill was used to make the curved edges, reference 1 in the graphic below, to prevent the need for an additional fixturing.

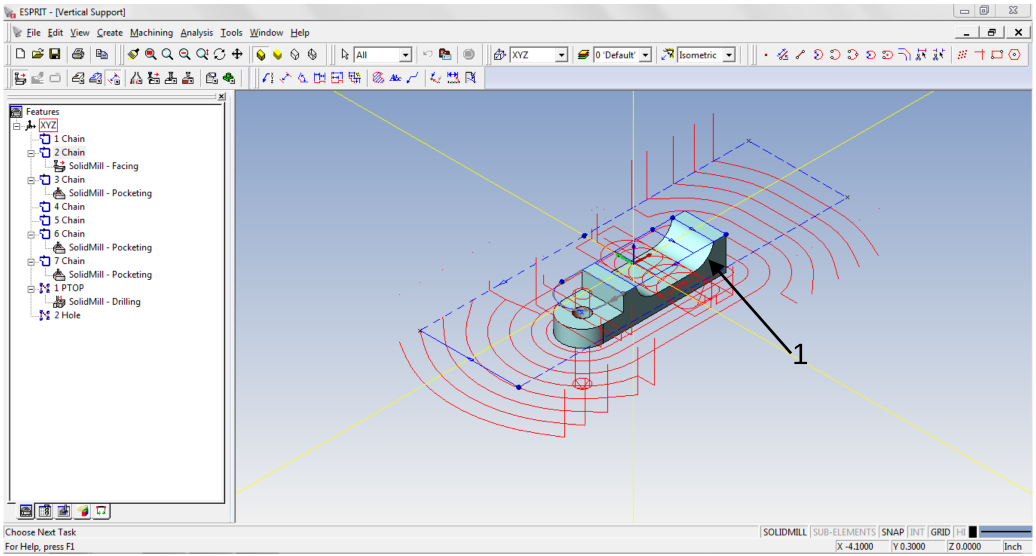

Figure 23: Screenshot of ESPRIT

The VM-2 runs at twice the RPM as the MiniMill; therefore, it is able to facilitate faster machining. The probe for the VM-2 is also in better condition than the MiniMills. For these reasons the VM-2 was used to make complicated parts and fine tune bearing holes for press fits. In Figure 24, the stock material is shown on the right and the base is shown on the left. To reduce the spindle load the step over was set to 30% of the max for the endmill. A sacrificial piece of metal was used as a fixturing point to make the base, top cross, and the top. The sacrificial metal was required to be rotated 180 degrees while making the base; thereby effecting the relation between the holes and the remaining cuts by 3 mm. The holes are used to attach the link collar. Only the position of the arm in relation to the joint was affected.

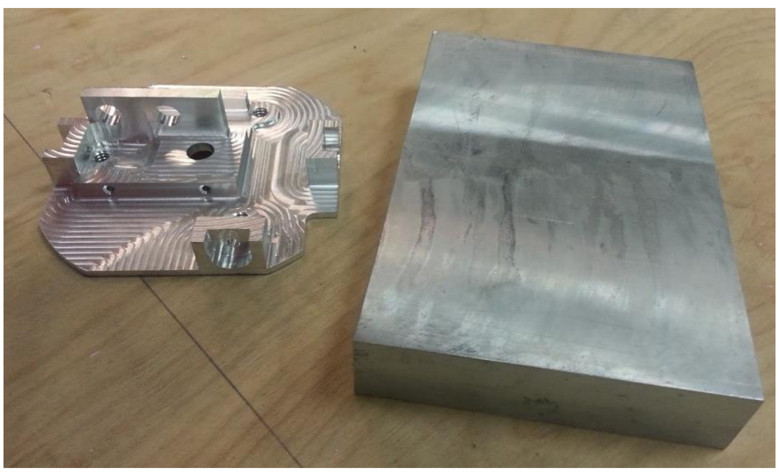

Figure 24: Machined base piece next to stock aluminum block

To assure that no preloading would result from assembly the top screw holes on the vertical supports were not drilled and tapped until all other components were assembled. The complex geometry of the parts resulted in burs from machining not being able to be removed using a de-burring knife. Sand blasting the components removed all burs, resulting in a safe to handle assembly.

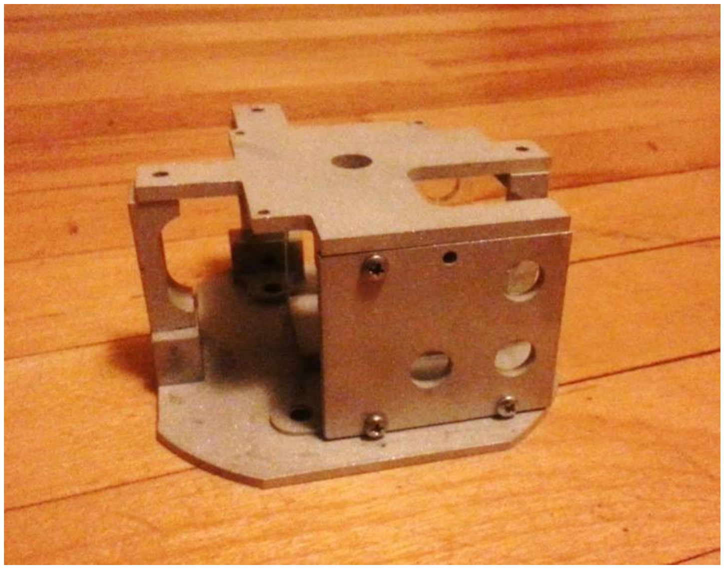

Figure 25: Assembled aluminum components

4.2 Electrical Design

Before designing the electrical system for the modular joint, several requirements had been decided upon based on the initial requirements for the project. The electrical requirements are listed below:

- The motor shall be able to generate enough power to rotate the joint at the minimum speed of 45 degree per second through gear reduction and be able to lift a mass of 1kg at 1 meter from the axis of rotation.
- The motor driver shall provide enough current to power the motor.
- The joints shall operate from a 12V DC power source.
- The encoder shall be able to detect the joint movement with a precision of 1 degree.
- The limit switch shall set the range of motion to at least 180 degrees.
- The microcontroller shall be able to read in the sensor data, receive the data from the controller, calculate the PID algorithm, and output the PWM signal.
- The control circuits shall be integrated within the joint.

The electrical diagram that is shown in Figure 26 below was initially designed to demonstrate the electrical system of joint. From the diagram we can see all the joints are connected with one serial I/O line and one power line. The serial I/O line provides data communication between base and joints. Each joint has an individual microcontroller that connects to an encoder and motor controller. The encoder is physically mounted on the rotational shaft to provide positional feedback. The microcontroller then compares the position feedback with desired position and calculates the speed of motor using a PID algorithm.

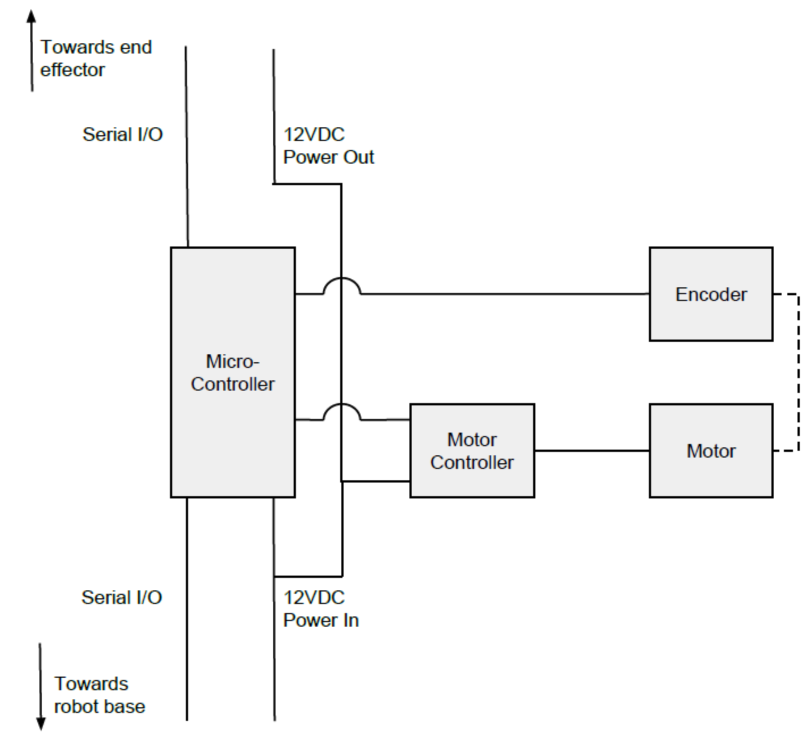

Figure 26: General electrical system diagram

Component Selection

Motor Selection

In order to select the motor that best fits the requirement, the team calculated the required motor power based on the task specifications. Assuming we have a three linked robotic arm with two pitch joint J1 and J2 as shown in picture below.

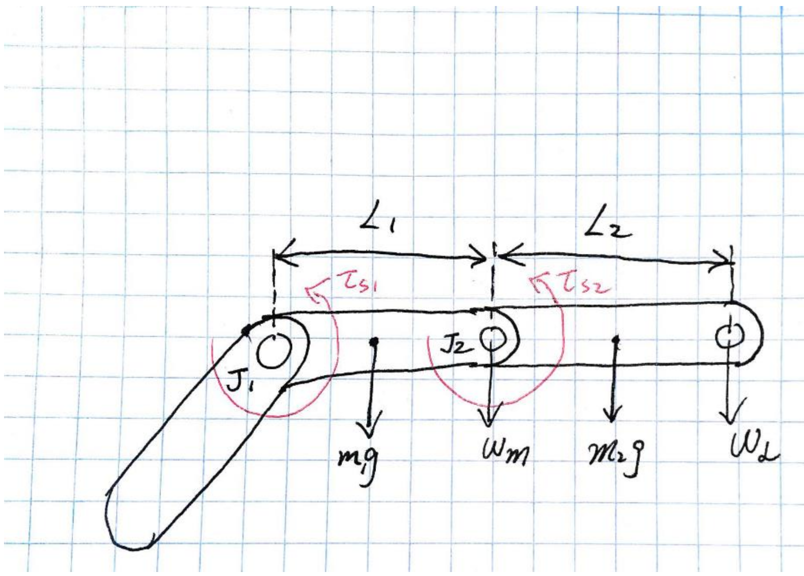

Figure 27: Free body diagram of a 3-link planar robotic arm

The equation to calculate the static torque for two joints is shown below:

$$T_{s1} = m_1 \cdot g \cdot 0.5 \cdot L_1 + W_l \cdot g \cdot (L_1 + L_2) + m_2 \cdot g \cdot (L_1 + 0.5 \cdot L_2) + W_m \cdot g \cdot L_1$$
$$T_{s2} = m_2 \cdot g \cdot 0.5 \cdot L_2 + W_l \cdot g \cdot L_2$$

Figure 28: Static torque calculation equation

Based on our requirement, the robot should be able to lift up 1 kg weight at the distance of 1 meter with the speed of 45 degree/s, which is 7.5 rpm. The maximum weight of each joint should be no heavier than 0.5 kg. The PVC pipe we are going to be using weighs about 0.42 kg per meter and each link will be about 0.5m long. With the following values:

$$L1 = L2 = 0.5\,m$$
$$m1 = m2 = 0.21\,kg$$
$$Wl = 1\,kg$$
$$Wm = 0.5\,kg$$

We then calculated:

$$Ts1 = 14.31\ Nm$$
$$Ts2 = 5.41\ Nm$$

Since the joints are the same for robotic arm, we choose Ts1 as the maximum torque arm needs to provide. As shown in the torque-speed graph of motor below, in order to run a motor in its maximum efficiency, the speed should be running around 70%-90% of the no load speed and the torque should be around 10%-30% of the stall torque [19].

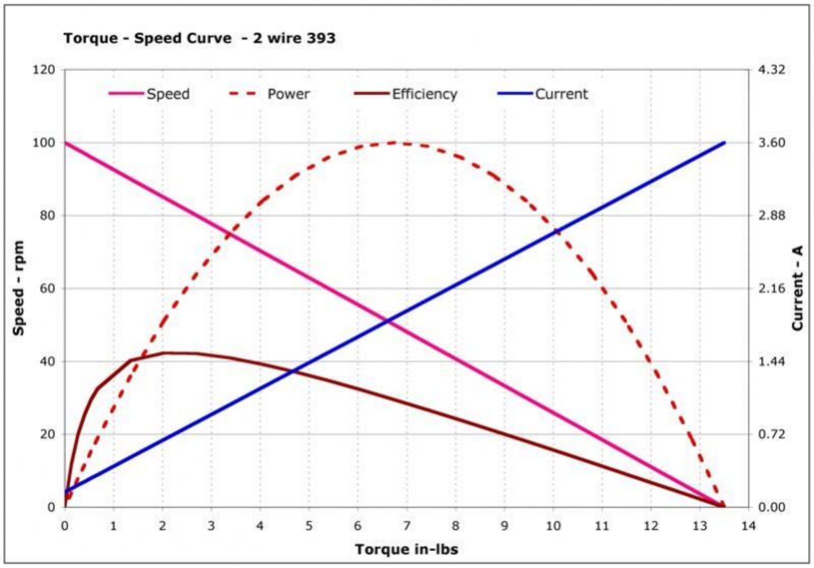

Figure 29: Torque-speed curve of a DC motor [20]

Thus, we can estimated the stall torque to be around 71.55Nm and the speed to be around 9.4 rpm.

We then calculate the maximum power needed to lift the weight. The maximum power can be calculated by multiplying half of stall torque and half of the no load speed, as shown in equation below:

$$P_{max} = \frac{T_{stall}}{2} * \frac{S_{maxrpm}}{2} / 9.5488$$
$$= \frac{71.55\ Nm}{2} * \frac{9.4\ rpm}{2} 9.5488 = 17.6\ W$$

We calculated the maximum power is around 17.6W. Because the motor loses power during operation, we need to give a safety factor of 1.5 to assure the right amount of power needed; therefore, the motors that fill our requirement need to have power at least 26.4W.

Motor Driver Selection

To drive the brushless motor, the team decided to use electronic speed control, or ESC. It is an electrical circuit used to control the direction and speed of brushless motor. ESC controllers are often used by model hobbyists in radio controller model planes and cars.

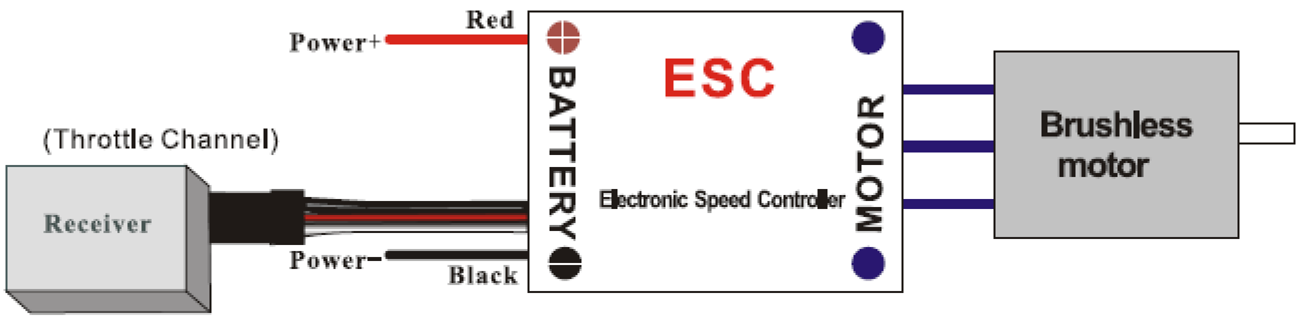

Figure 30: ESC wiring diagram [21]

As shown in Figure 30 above, the ESC is powered by external battery. The battery type can be Li-ion or NiMH. It has three wires connected to receiver which are ground, power, and signal. In our application, the three wires will be directly connected to microcontroller. Most ESCs have built-in battery eliminator circuit (BEC) that can provide 5V power through a power line. It is an electronic circuit used to provide electrical power to other circuit without the need for a battery. 5V is used to power the microcontroller. The microcontroller then sends a PWM signal through signal line to control the direction and speed of motor. On the right side, the ESC provides three-phase power to drive the brushless motor.

In order to provide enough current to drive the motor without damaging the ESC, the appropriate ESC must withstand continuous current that is larger than the motor's maximum current, which is 12A. Initially, the team chose an Exceed RC Proton 12A brushless ESC which is able to withstand continuous current up to 18A. The input voltage can range from 5.6V to 16.8V. However, when testing the ESC we realized that Exceed RC Proton 12A brushless ESC did not support reverse motor direction because this controller was designed to be used on RC planes to rotate the propeller, which only rotate in one direction. Through research on the Internet, we found out an ESC used on RC cars has the mode to allow the motor to rotate in both directions.

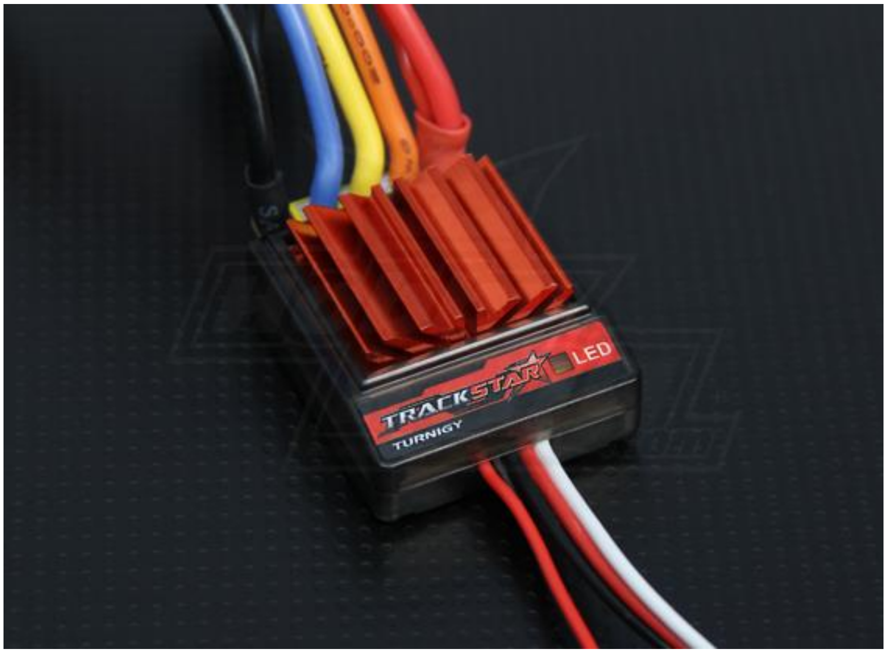

Figure 31: Turnigy TrackStar 25A ESC [33]

The team soon found that the Turnigy TrackStar 25A brushless car ESC (shown in Figure 31) can provide continuous current up to 25A and is able to reverse the motor direction. This ESC has BEC that provides 5V/1A output to microcontroller.

Encoder Selection

In a close-loop system, an encoder plays a significant role by providing feedback data into the system. There are many existing encoders on the market and they are categorized in two types, incremental encoders and absolute encoders. Incremental encoders provide a series of periodic signals when motion occurs. The number of cycles corresponds to the increments of motion. Many incremental encoders are two-channel, meaning that there are two output signals and the two signals are offset by one cycle. Two-channel outputs allows encoder to detect the direct of motor. Absolute encoders provide unique output for every position in the range of motion. Therefore the output corresponds to the position. Initial research determined four encoders of either type that would work, as shown in the table below.

Name	Picture	Company	Price	Type	Resolution	Shaft Diameter
E4T OEM Miniature Optical Kit Encoder		US Digital	$39	Optical Miniature Encoder	300 cycle/rev	6.35 mm
ENC300 CPR Easy Roller 300 CPR Quadrature Encoder		Solutions Cubed	$35	Quadrature Encoder	300 cycle/rev	2 mm
MAE3 Absolute Magnetic Kit Encoder		US Digital	$69	Magnetic Absolute Encoder	4096 position/rev	2 - 6 mm
AEAT-6010-A06		Digikey	$25.68	Magnetic Absolute Encoder	1024 position/rev	6 mm

Table 8: Encoder Selection [22][23][24][25]

The first two encoders are both 2-channel quadrature encoders and have 300 cycles per revolution. The last two encoders are both magnetic absolute encoders. The First one has 4096 position per revolution, which is four times of the resolution than the second. The first also has the price that is almost three times higher than the second one. In the design requirements, the tolerance of angular position should be within 1% of the full rotation of the joint, which is 3.6 degrees. The 1024 position per revolution can measure 0.35-degree position, which is much more accurate than the requirement states. The team decided to use AEAT-6010-A06 magnetic absolute encoder.

Electrical Connections

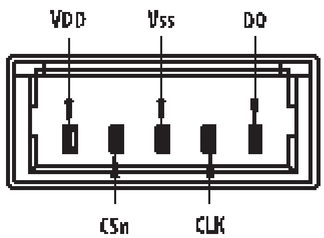

Pin	Symbol	Description
1	VDD	5V Supply Voltage
2	CSn	Chip Select – Input (See Figure 2)
3	VSS	Supply Ground
4	CLK	Serial Clock - Input (See Figure 2)
5	DO	Serial Data - Output. (See Figure 2)

Figure 32: Encoder Electrical Connections [27]

As shown in figure above, AEAT-6010-A06 magnetic absolute encoder has five connections, which are 5V supply voltage (VDD), chip selection (CSn), supply ground (Vss), serial clock (CLK), and serial data (DO).

Communication Protocol

Among all different types of serial communications, the Inter-Integrated Circuit (I^2C) communication is the most efficient and uses the least physical communication ports. I^2C allows multiple slave devices to communicate with one or multiple master devices. It was designed for a short distance communication. I^2C uses two wires (SCL and SDA) to communicate, SCL synchronizes the clock and SDA transmits data. The protocol supports up to 1008 devices to interconnect and communicate at a rate up to 400kHz [26]. Figure 33 demonstrates how multiple joints could wired in parallel using I^2C communication.

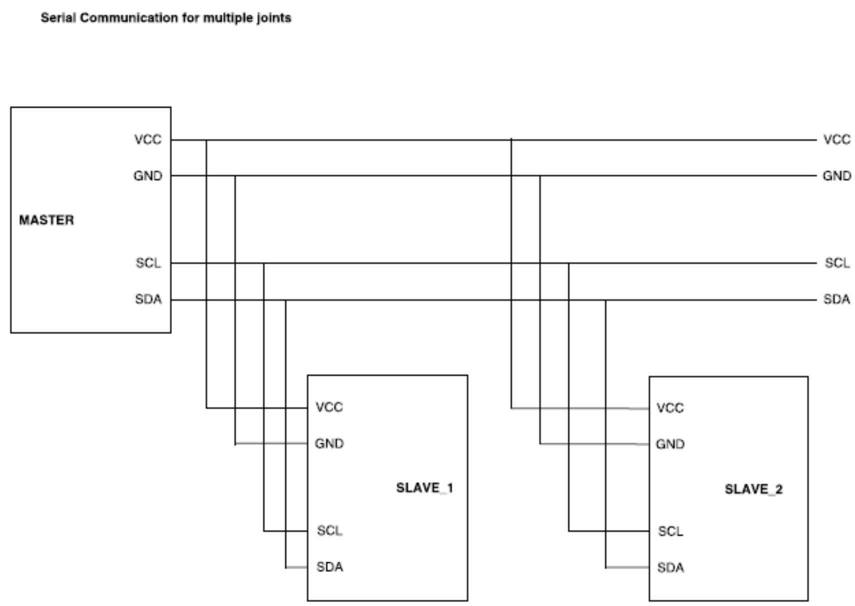

Figure 33 Diagram demonstrating how multiple joints could be wired in parallel [26]

Microcontroller Selection

To select the microcontroller that best fit requirements as well as being low-cost, the team created a detailed functional diagram of a joint's internal electrical components, which can be seen in Functional Diagram section. As discussed in the previous section, an ESC has a three-pin connection to a RC receiver, which in our case was replaced by microcontroller. The three pins were 5V power output, ground, and PWM signal input, which can be connected to a digital IO port on the microcontroller. The absolute encoder we selected has five-pin connector shown in Figure 34 below. Chip Select, Serial Clock, and Serial Data were connected to IO ports on microcontroller. The limit switch required one digital IO port and ground. To communicate with main board, we used I^2C communication which requires two ports. Through researching, we found Arduino Pro Mini 328 5V/16MHz that fit all the minimum requirement and has a relatively small 18x33mm size.

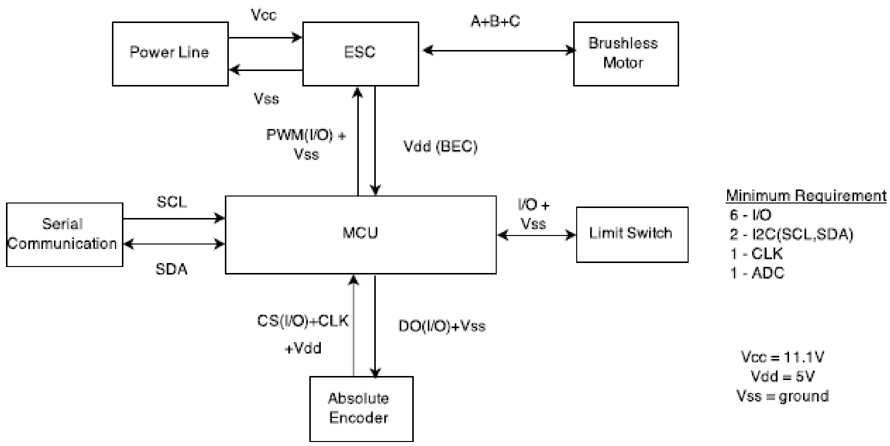

Figure 34: Functional diagram of a joint's internal electrical components

Schematic Design

After selecting all the electrical components, we designed a schematic sheet for the joint circuit as shown in Figure 35. The schematic was designed based on the specification of pins on the Arduino Pro Mini. To eliminate the signal noise of the limit switch, we added a signal debouncing circuit between limit switch and digital IO port on Arduino Pro Mini. To ensure the constant 5V power input, we connected a 0.1μf capacitor between ESC power line and Vcc on Arduino Pro Mini.

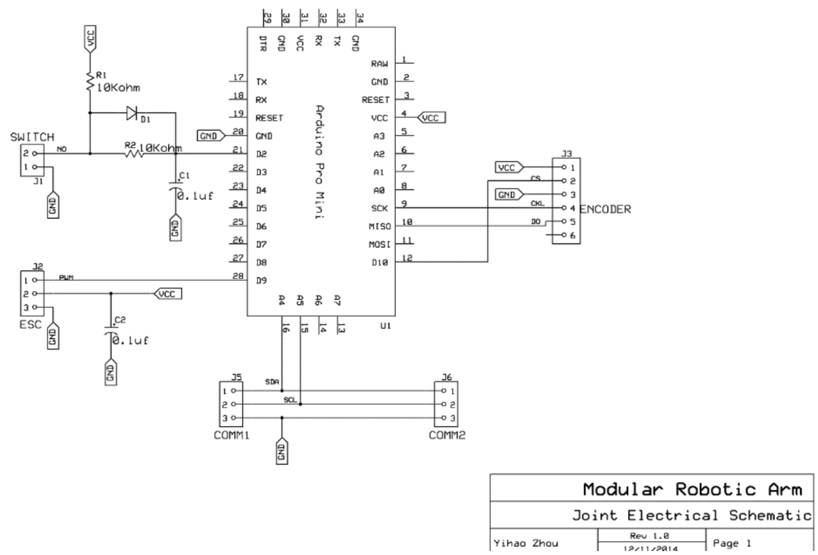

Figure 35: Arduino pinout diagram

PCB Design

After completing the schematic design, we designed a PCB board using ExpressPCB software based on the schematic sheet. As shown in Figure 36, the overall board size is 35mm by 35mm. There is a circular hole in the middle of the board to allow shaft to pass through. The board is mounted on the top cross of the joint. The black lines are the wires that connect all the pins. The thin lines are the signal wire. The thicker lines are the power and ground lines because they have more current going through than signal lines.

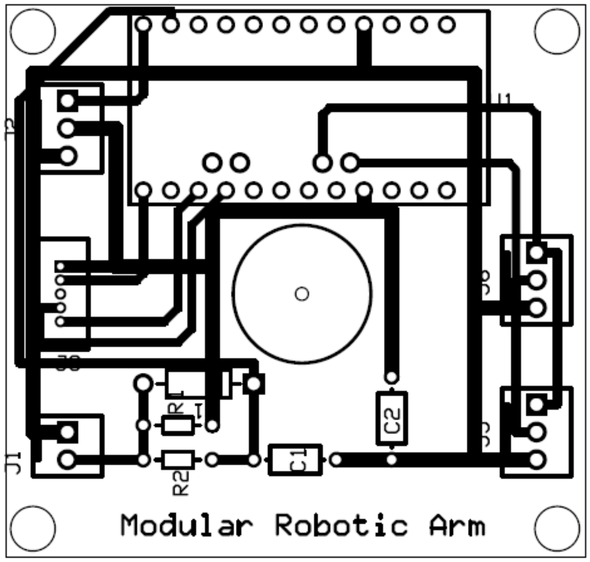

Figure 36: PCB diagram

4.3 Programming Design

The programming design of the modular robotic arm system can be separated into three modules, which are the program on the joint to control the rotation, the program on the main board to distribute the position data to the joints, and the program on the computer to interact with users. The general requirement for the program are:

- The user shall be able to plug in the main board into computer and control the robot arm using any interactive user interface
- The robot arm shall be able to automatically rotating and moving to target position once receiving the command from computer

The detailed programming requirements were:

- There is a simulation of the arm in the computer for the user to interact with
- Software needs to use inverse kinematic tool to convert the target position to the rotational angle for each joint
- The master board takes the rotation data of all the joints and distributes to each joint through I2C and waits for response
- When each joint receives the data, it starts PID controller to control the movement
- Once the joint reaches the target angle, the joint will send back to main board the actual angle and success message. If the joint fails to reach the target angle, it will send the actual angle and a failure message
- Once the main board receives the failure message, it will terminate the action and send error message to computer.
- The computer will display the error message to users.

Program Flow Chart

Figure 37 shows the flow chart of main controller unit. As shown in the graph, the initialization function is first called. In the initialization function, the system first checks the status of all the joints. Then it reads in the actual position for each joint and set default target position same as actual position. Finally, the system starts timer interrupt. In the interrupt service routine, the system first requests the actual position from each joint. If the system receives the actual position data from joint, it updates the local actual position data as well as sending actual position data to PC. The system then request target position data from PC. If the system receives the target position from PC, it updates the local target position data as well as sending the data to the joint.

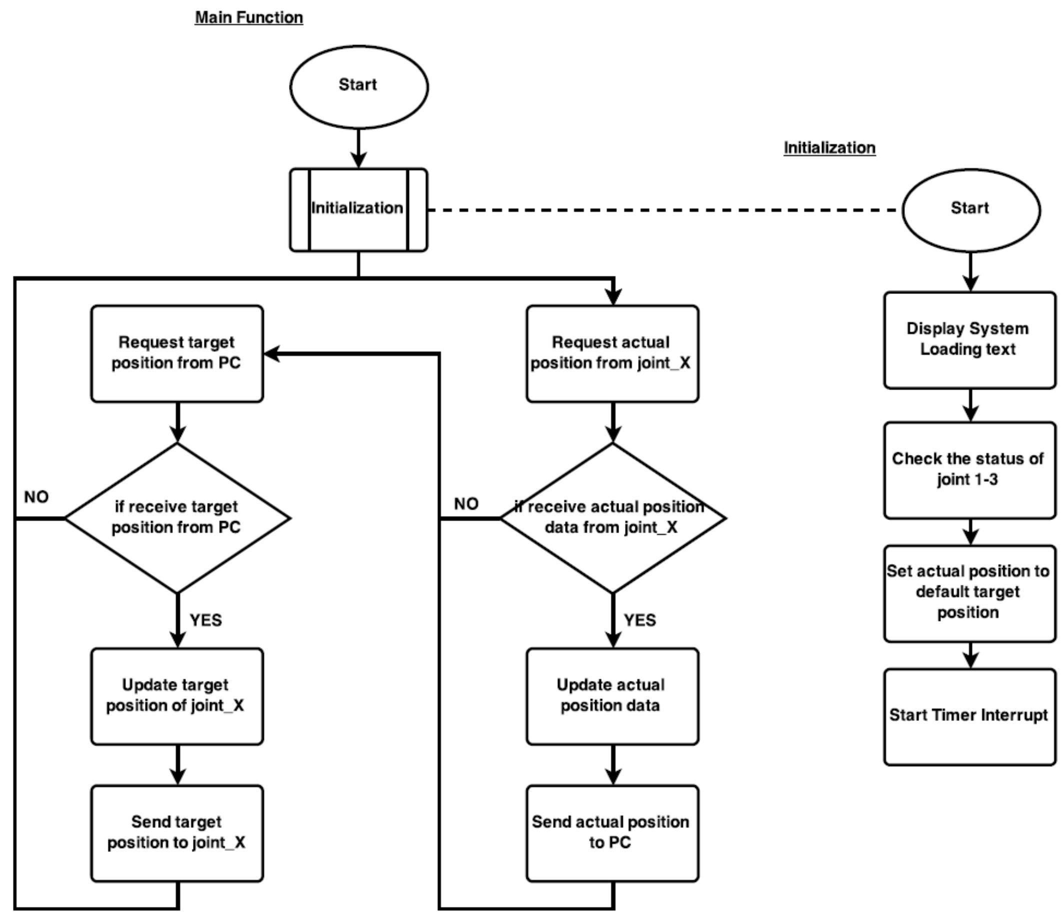

Figure 37: Main Controller Flow Chart

Figure 38 shows the flow chart of the joint controller unit. Once the program starts, it first checks if the limit switch has been pressed or not. If the limit switch is not pressed, the system starts to read in the encoder value and set the value as the input for the PID algorithm. Then the system computes the output value using the PID algorithm. The output value is the speed to drive the motor. The joint controller program has two I2C interrupts that are called when the main controller requests for the actual position data or when the joint controller receives data from the main controller. When sending data to the main controller, the program parses in encoder value as a 2 byte package and then sends to the main controller. When receiving the 2 bytes data from main controller, the joint controller parse in the data as the set point for PID algorithm.

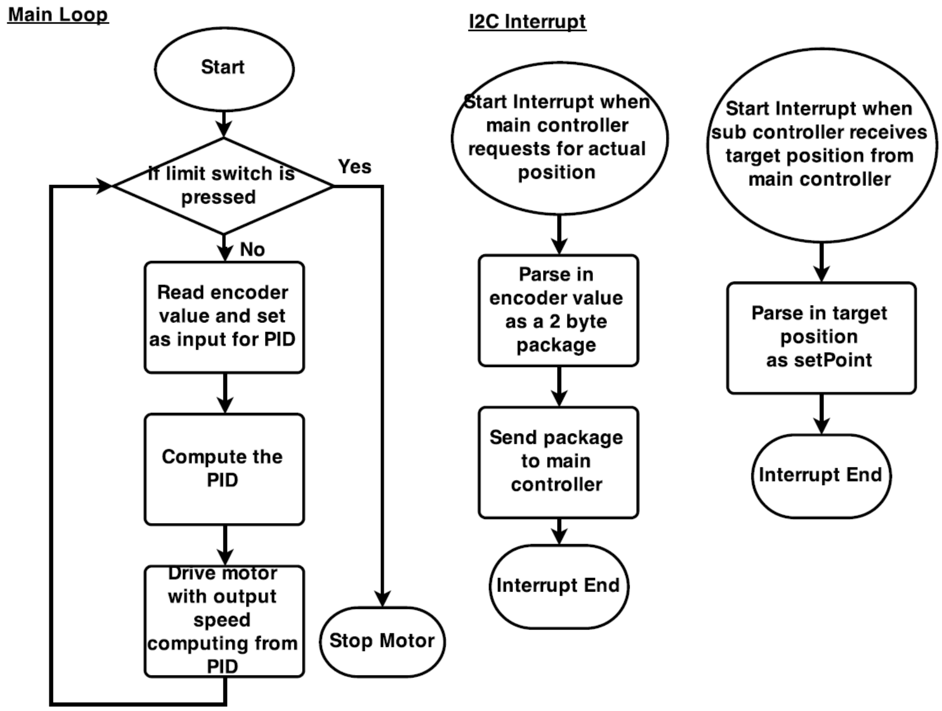

Figure 38: Sub Controller Flow Chart

4.4 Summary

Following a systems engineering approach the team designed a joint that was analyzed using simulation packages in SolidWorks. The team also designed the customized electrical system for the joint and wrote programs to control multiple joints.

5. Results

5.1 Introduction

As each subcomponent of the joint was completed, various levels of testing were run to ensure that the final joint would behave as per our task specifications. The electrical and software subsystems were the first to be completed followed by the mechanical components.

5.2 Results

Mechanical Results

In the end, we were able to machine or purchase all of the necessary mechanical components. These can be seen in Figure 39.

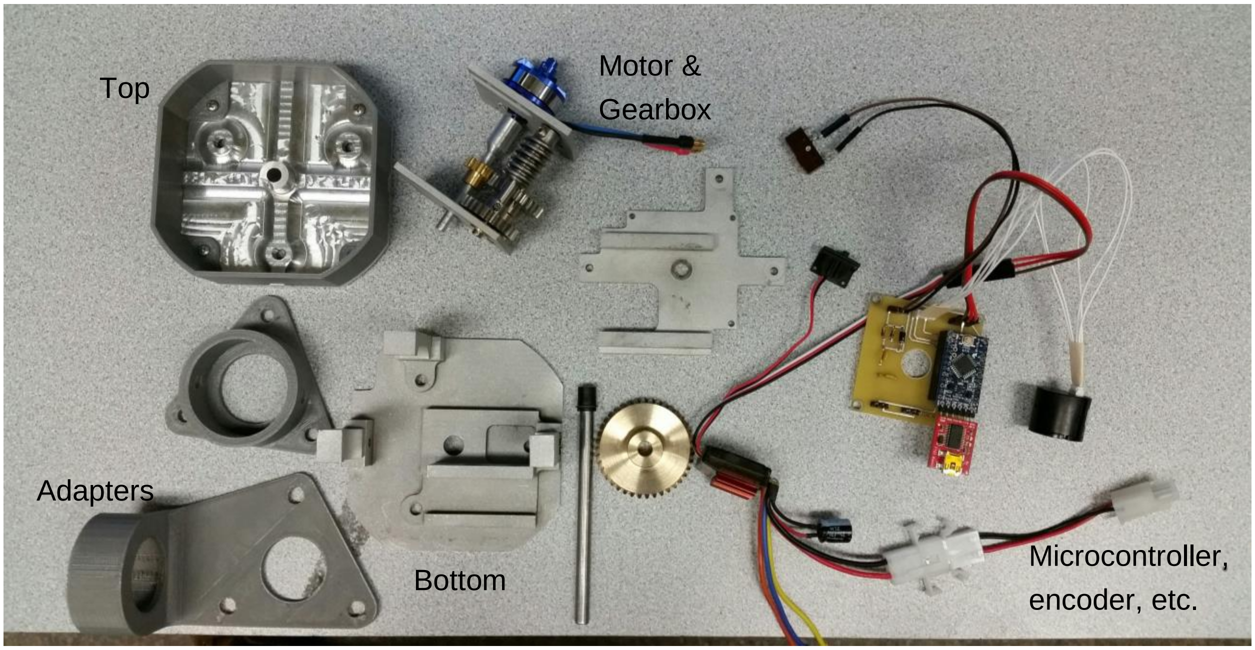

Figure 39: The mechanical and electrical components of the modular robotic joint

The most significant obstacle in implementing the mechanical systems was dealing with the tolerances needed for the gearbox to work properly. In an earlier 3D printed version of the joint, the tolerances produced by the 3D printer were not sufficient to test the design. The shafts ended up misaligned to the point where the gears could not rotate freely even without a load. At the time, the proposed solution was to create the parts out of aluminum for the final version which would have tighter tolerances and would be able to operate correctly.

During the manufacturing process of milling the various parts out of aluminum, it was discovered that the tolerances from WPI's CNC machines were not much better than those of the 3D printer. We speculate that the reason for this is that the machines have lost their precision due to improper use from students learning to machine on them.

In order to get the gearbox to operate correctly, several modifications were made. The hole on the plate which held the brushless DC motor had to be enlarged to fit the shaft and the mounting holes needed to be repositioned. On the other bearing plate, two of the bearing holes were too close together forcing two gears into each other and preventing rotation. This was solved by replacing one of the bearings with a bushing which was then drilled into and enlarged to allow the gear shafts to be further from each other.

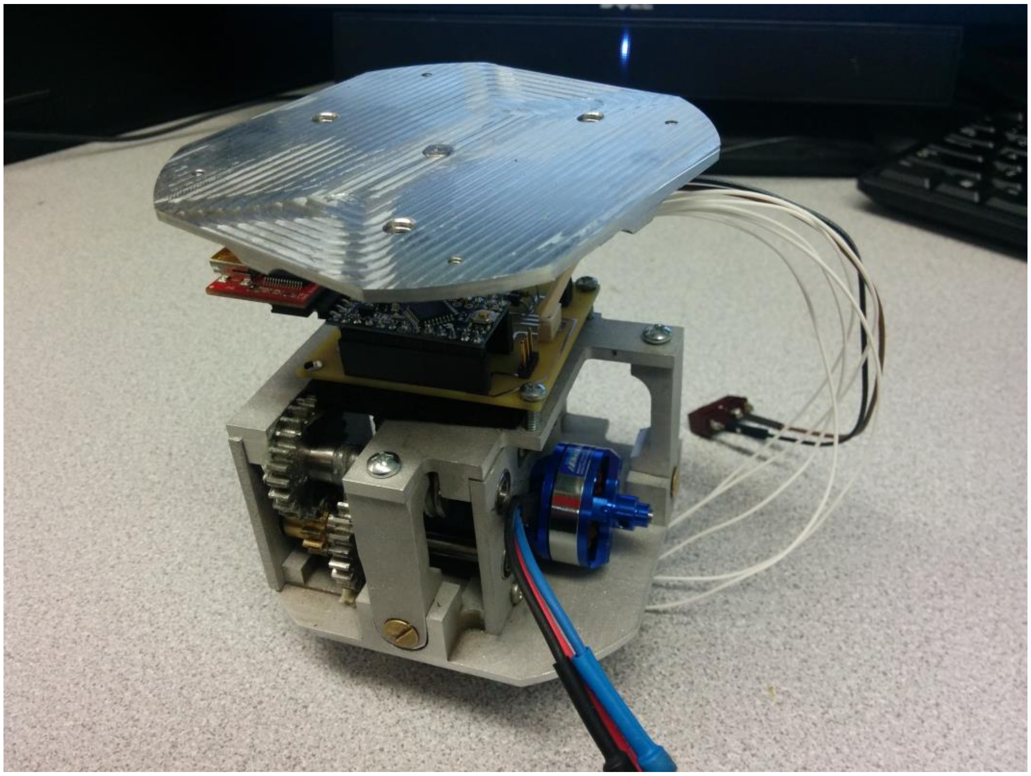

Figure 40: The assembled modular robotic joint

When finally assembled as shown in Figure 40, the output shaft rotated with an input rotation from the motor as designed but was not without much friction between the gears. This led to the gear train not rotating as smoothly as desired, even with ball bearings, which could potentially reduce the output torque to the output shaft.

Electrical and Programming Results

After the designing the customized circuit board, we ordered a PCB from a circuit printing service, ExpressPCB. Once the printed circuit board was delivered, we soldered all the components onto the circuit board and tested the functionality of each component separately.

We first tested the debouncing circuit for the limit switch by programming a simple Arduino program that would print to the serial monitor “0” when a switch was not pressed and a “1” when switch was pressed. Then we tested the PWM port. We used a power generator to provide a 12V output power to the ESC controller. Because the microcontroller was powered by a computer via USB, we did not need the ESC to provide 5V BEC power. Therefore, when connecting the ESC with the circuit board, we only connected the PWM signal and ground wires, leaving the power wire disconnected. We then programmed a simple Arduino code that varied the PWM output value between 1000 and 2000. The motor was able to spin at different speeds and directions. The motor spun forward at maximum speed when setting value to 2000. The motor spun backward at maximum speed when setting the value to 1000. The motor stopped when the value was set to 1500. We also tested the encoder by writing code that triggered a clock signal every 50 milliseconds and printed the value that was read from encoder to serial monitor. As the result, the encoder was able to send the values from 0 to 1023 when rotating the shaft from 0 to 360 degrees. Finally, we tested the I2C communication between the joint circuit board and main board. We used an Arduino Uno as the main board and connected it to our customized circuit board using two jumper wires. The Arduino website provided a library specifically for I2C communication, which we used for our serial communication between the two boards. We were able to successfully send string data from the main board that was then received by the joint board as well as send string data from joint board and have it be received by the main board.

Integrated System Testing Results

ID	Need	Description	Final Result	Explanation
N 01	**Modular joints**	All joints should be able to be used in combination with any other joint(s)	Each joint contained all necessary parts to operate alone yet was able to interface with others	Through adapters, each joint was able to connect mechanically to any other in series. Due to the serial connections, each joint could receive its own designated commands and operate independently
N 02	**Payload**	A joint should be able to lift a 1 kg load held at one meter horizontally from the axis of rotation	This was not tested but is potentially not possible due to poor meshing and internal friction of the gearbox	The adapters which would allow the joint to connect to an arm-piece and lift a weight were 3D printed due to time constraints and are unable to hold the necessary torque unlike a piece machined from aluminum
N 03	**Rotational velocity**	While under no load, each rotational joint should be able to rotate at at least 45 deg/s	This has been tested running motor under full speed. The joint is to rotate 60 deg/s.	The motor is able to reach the required velocity. However, due to the friction between gears, the motor needs to be running under full speed to be able to rotate smoothly
N 04	**Rotational velocity under load**	A joint should be able to rotate at a minimum of 45 deg/s while holding a 1 kg load one meter horizontally from the axis of rotation	This was not tested but is potentially not possible due to poor meshing and internal friction of the gearbox	The adapters which would allow the joint to connect to an arm-piece and lift a weight were 3D printed due to time constraints and are unable to hold the necessary torque unlike a piece machined from aluminum
N 05	**Motion constraints**	The joint should not interfere with the range of motion of other joints on the arm	This was designed but not tested	Since only one joint was fully manufactured, multiple joints could not be tested together though through simulating Solidworks assemblies, this task spec is believed to have been met
N 06	**Length of joint**	Each fully extended joint should be approximately 15 - 20 cm long	The final joint measured 9.29 cm in height and 10.8 cm in diameter at its widest point without the attached adapters	Through the use of a relatively small brushless DC motor and a custom gearbox, we were able to stay below our desired demensions
N 07	**Wire Safety**	The wires on the arm should present no safety hazard. Including, areas where fingers could be crushed	This was met individually by each joint but not when assembled into an arm	Each joint contained all its necessary wiring within its shell. The wires to connect each joint to each other however, need to be run along the outside of the arm pieces instead of internally
N 08	**Cost**	The price of materials for each joint should be no more than $150	Though difficult to give a final cost, it is believed that each joint would cost approximately $400 without a profit margin if mass produced	Much of the aluminum stock was salvaged from other projects and all of the machining was done within WPI's machine shop meaning that the only cost involved was time. Estimates were gathered from local machine shops though which gives us an approximate total cost

Figure 41: Comparison of design specifications to the final results

ID	Need	Description	Final Results	Explanation
N 09	**Accuracy**	Any rotation to a software defined angular position should be within 1% of the full rotation of the joint	This is achievable through the use of the built-in absolute encoder along with proper PID setup	The encoder used was 10-bit meaning that it was able to measure accurately to within approximately 0.352 degrees of rotation. This coupled with proper PID values would allow a user to attain this accuracy
N 10	**Precision**	Any three consecutive rotations to the same software defined angular position should be within 1% of the full rotation of the joint	This is achievable through the use of the built-in absolute encoder along with proper PID setup	The encoder used was 10-bit meaning that it was able to measure accurately to within approximately 0.352 degrees of rotation. This coupled with proper PID values would allow a user to attain this precision
N 11	**Maximum weight**	Each joint should not weigh more than 0.5 kg	The final joint weighed 0.584 kg without the adapters or outer shell	The structural strength of each joint was much more than sufficient for the potential loads on the joint meaning much excess material remained, which added extra weight. Removing this extra weight would have proven a difficult machining task though
N 12	**Range of motion**	A pitch joint should be able to rotate at least 120 degrees. A roll joint will be able to rotate at least 180 degrees	Each joint could rotate 270 degrees	Since each joint could fulfil the role of both a pitch joint and a roll joint through the use of adapters, all joints retained the same freedom of rotation. The design and mechanical dimensions of the adapters allowed for at least 270 degrees of rotation
N 13	**Power supply**	The joints should operate from a 12 VDC power source	Each joint operated off of a 12 VDC power supply	The voltage and power requirements of the electrical components were selected such that each joint would operate off of 12 VDC
N 14	**On board electronics**	Each joint should contain a microcontroller and sensors needed to accept positional input and move to the desired position within the defined accuracy	Each joint contained the necessary electronics and sensors to achieve this	The only input requirements to each joint are a power source and a serial command. Each joint is then able to handle motion on its own based on these

Figure 42: Comparison of design specifications to the final results [con't]

Thermal Analysis

When designing an electromechanical system, analyzing the thermal properties of the system is important in ensuring the device works properly. This is because electrical components have operating temperatures which, when exceeded could cause failure of the circuit while structural materials can be weakened and melt at higher temperatures.

For our modular robotic arms joint, excessive heat could be a potential issue for several components. Key amongst these was the Arduino Pro Mini whose Atmel microcontroller has a rated temperature range of -40℃ to 85℃ [30]. The PLA (Polylactic acid) plastic used for the outer shell of is also of concern with regards to its temperature. At 60-65℃ PLA undergoes glass transition meaning it becomes softer and rubber-like [31]. At 173–178℃, PLA will begin to melt. Because of this, our ideal maximum temperature achieved inside of the joint would be below 60℃ while temperatures up to 85℃ could be tolerated as the PLA plastic does not comprise any of the structural elements within the system.

The components that could create the most heat within the joint are the motor controller and motor with the Arduino generating a slight but likely negligible amount of heat. By comparison, the Exceed RC Rocket brushless motor used in our system consumes up to 90 Watts of power when under load [32]. Its maximum efficiency is listed at 75% meaning that while consuming maximum power, under ideal efficiencies, 22.5 Watts is lost due to heat and radiation.

In order to power the brushless motor, a Turnigy TrackStar 25A brushless motor ESC was used. This motor controller can provide continuous current up to 25A and bursts of up to 90A [33]. The motor controller comes with a built-in heatsink meaning that heat generation and dissipation is a legitimate design concern.

To assure that performance issues would not arise due to heat building up inside the joint, ANSYS Workbench was used to perform a thermal study on our joint. The first step in this analysis was to create a simplified Solidworks model of the joint in order to make thermal simulation easier. The critical components were kept such as the motor and motor controller but parts such as the outer shells were combined into a singular piece and some of the details of the base and top were removed. This can be seen in Figure 43.

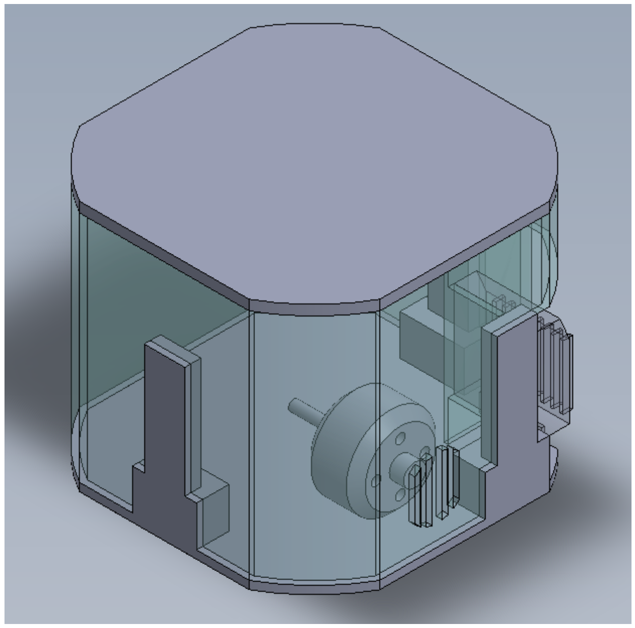

Figure 43: Simplified joint for thermal analysis

This model was then exported from Solidworks and imported into Workbench. Within Workbench the various material properties were set such as material type. For the outer shell, polyethylene was used instead of PLA plastic. Since Workbench did not contain PLA within its library of materials, polyethylene was a good substitution and a material that could potentially be used in a more mass produced version of the joint since 3D printing is not ideal for mass volume production.

Convection, internal heat generation, and initial temperature conditions were all set for the various components within the assembly. In the simulation seen in Figure 44, the ambient temperature was set to 22°C, slightly below room temperature. The base, shell, and top parts each began at 26°C to simulate having already been heated above the ambient temperature. The motor and motor controller were both set to 50°C in order to simulate having been heated by operation. These are temperatures which could be realistically seen from these components.

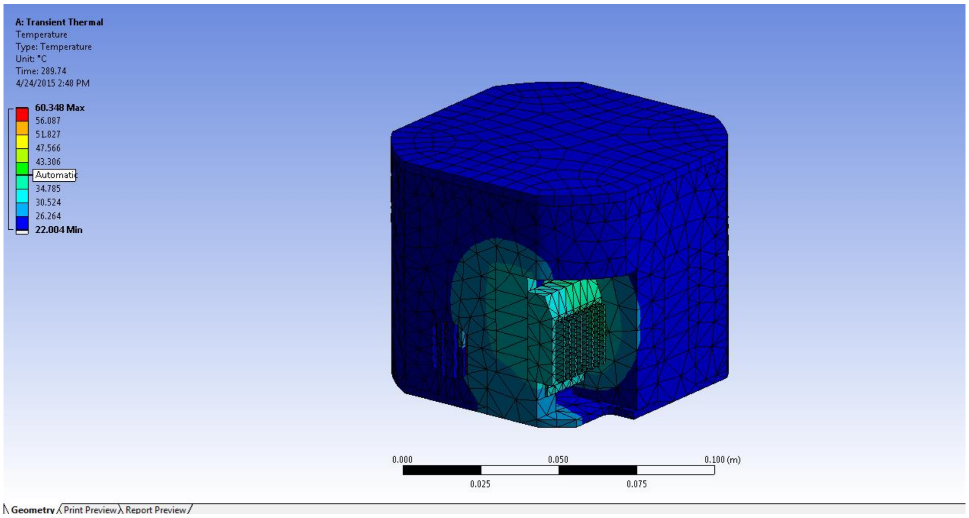

Figure 44: ANSYS Workbench thermal simulation

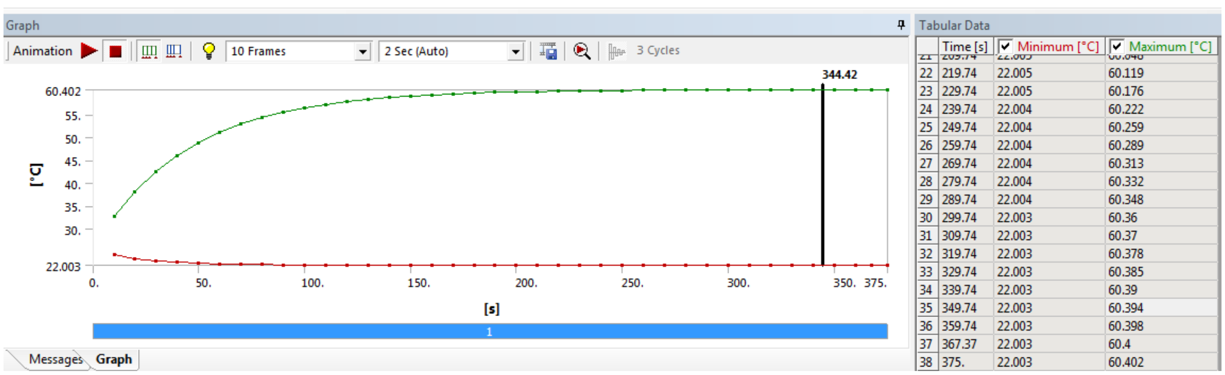

Figure 45: ANSYS Workbench temperature vs. time graph

Based on the part specifications, the heat given off by the motor would be 22.5 Watts under ideal conditions. This heat generation was also defined within Workbench. Convection and conduction coefficients based upon individual material properties were also taken into account.

The results seen from this simulation show that the hottest components in the system reach a steady state temperature of about 60°C as shown in Figure 44. Though this result is under ideal heat dissipation and motor heat generation conditions, this steady state takes approximately 250 seconds to achieve meaning that the motor would have to operate for that long under maximum load to reach these temperatures. This is unrealistic as the motor can only rotate for a limited amount of time before reaching the rotational limits imposed by the geometry and limit switches of the joint. The joint would also need to be supporting a kilogram at a meter from the axis of rotation horizontally for the current draw to rise high enough to generate the 22.5 Watts of heat. Because of the simulation as well as these reasons, heat dissipation within the joint does not appear to be a concern. Though only an approximation, the maximum temperature simulated is 25°C below the maximum limit of 85°C for the electrical components and takes too much time to reach to be an issue.

5.3 Summary

Most of the design specifications defined at the beginning of the systems engineering process were met by the final iteration of the joint. Most of the issues arose from the precision of the machining equipment used to manufacture the joint. The joint was successful however in proving that the original objective could be realistically met through future iterations of this project.

6. Summary and conclusions

6.1 Introduction

The final implementation of the modular robotic arm joint proved mostly successful though not entirely as imagined. The reasoning, issues encountered and recommended future work can all be seen in the sections below.

6.2 Summary of System Design and Results

The joint created by our group consisted of a single degree of freedom modular arm system. With adapters, a user would be able to connect multiple joints together by using SCH80 PVC pipe which would be easy to cut to a custom length. Each joint then only requires power and an I^2C serial message to operate. In this serial message, a user can set the speed, position or PID values of the joint in order to control it.

6.3 Overall assessment

Summary of issues

The parts machined were small and complex. It required fixturing surfaces as small as $1cm^2$. The machine exerts large forces while milling away the material. These forces pushed the part out of the fixturing multiple times. To make the top part the Drill Mill Center (DMC) had to be used. The program was too large to fit on the MiniMills and the VM-2 was equipped for a five-axis lab for a class. The DMC does not have probing abilities; therefore, the tools were probed on the MiniMills and the numbers were transferred to the DMC. While making the top part the tool did not travel in the z+ direction enough to clear the part, resulting in a chipped part and a broken endmill.

Recommended future work

The two major improvements which could be made to this project are the machining process and the final weight of each joint. Besides these, the joint was able to meet its design specifications.

The tolerances of the final machined pieces proved to be inadequate to produce the gearbox as desired from the Solidworks model. Potential solutions to this include using better CNC machines, creating a design in which tolerances are less important or using other techniques besides milling parts from aluminum. The CNC machines available to our group have been used countless times by students learning to machine parts and have therefore lost their precision and accuracy over time from normal wear and tear. It is likely that our parts would have been better in terms of tolerances and accuracy had a newer machine been user or had a machinist with much more experience milled the parts. Due to the nature of our gearbox design, tolerances between and within parts was very important. If another design had been used in which tolerances were less important or had a premade gearbox been used, the operation of the final joint would likely have been improved measurably. Neither of these options seemed possible or viable for various reasons though during our design process. A final option would be to consider a different manufacturing process besides CSC milling. A 3D printed prototype was attempted but the same tolerance issues arose. It may be possible to use a higher quality 3D printer, potentially one which used better materials than PLA plastic, to create better versions of the required parts.

The weight of the final joint also proved to be an issue. Since our design specifications called for the joint to be able to achieve a certain desired torque, it is likely that the joint would struggle to move other joints connected further in series as well as a payload since a majority of power would be used to lift the weight of the joint. The current joint contains excess material which could be removed in future implementations while still meeting the required structural strength requirements. Another critical source of excess weight are the gears used in the gear train. The worm gear was made from brass which is much more dense than aluminum which could be a potential replacement material. The size of each gear could likely have been reduced as well in terms of both width and diameter. This would also have the added benefit of reducing the overall size of each joint.

6.4 Conclusions

While not every task specification defined at the beginning of this project was met, the final modular robotic arm joint proved that through future versions and iterations of this project, a modular arm system could be developed which could fill the market gap intended by this project. Through the use of better manufacturing techniques and lighter components, the results of this project could be improved with little time and effort. Our team was also able to use a systems engineering approach to simulate a real engineering design process and create a functioning robotic system. Because of these reasons, our team believes that we were successful in completing this project

7. Bibliography

[1] M. Quigley, A. Asbeck, and A. Y. Ng, “A low-cost compliant 7-DOF robotic manipulator,” in *IEEE International Conference on Robotics and Automation, 2011,* pp. 6051 – 6058.
[2] J. Baldiga, C. McCarthy, S. Fitzell, T. Watson, “Design of Low Cost Modular Robotic Manipulator Joints,” Worcester Poly. Inst. MA. 2009.
[3] Schunk. *Powerball Lightweight Arm LWA 4P* [Online]. Available: http://mobile.schunk-microsite.com/en/produkte/produkte/powerball-lightweight-arm-lwa-4p.html
[4] igus inc. *Robolink: Articulated joint modules for robots* [Online]. Available: http://www.igus.com/wpck/6658/robolink.
[5] *JACO 2 | Robotics [Online]. Available:* http://kinovarobotics.com/products/jaco-robotics.
[6] Magnet Man. “*Experiments with motors.*” [Online]. Available: http://www.coolmagnetman.com/magmotor.htm.
[7] Electical4U. *“Types of DC Motor Separately Excited Shunt Series Compound DC Motor.”* [Online]. Available: http://www.electrical4u.com/types-of-dc-motor-separately-excited-shunt-series-compound-dc-motor/.
[8] M. Brain. (2006, Dec. 15). “*How does a brushless electric motor work?*” [Online]. Available: http://electronics.howstuffworks.com/brushless-motor.htm.
[9] “Brushless DC electric motor,” in *Wikipedia, the Free Encyclopedia* [Online]. 2014. Available: http://en.wikipedia.org/wiki/Brushed_DC_electric_motor.
[10] “Stepper motor,” in *Wikipedia, the Free Encyclopedia* [Online]. 2014. Available: http://en.wikipedia.org/wiki/Stepper_motor.
[11] Dynetic Systems. “*Brushless vs Brushed Motors,”* [Online]. Available: http://www.dynetic.com/brushless%20vs%20brushed.htm.
[12] “Harmonic Drive,” in *Wikipedia, the Free Encyclopedia* [Online]. 2014. Available: http://en.wikipedia.org/wiki/Harmonic_drive.
[13] D. Ince, “Harmonic Drive,” in *A Dictionary of the Internet.* Oxford University Press [Online]. 2013. Available: http://www.oxfordreference.com.
[14] Z. Susman. ECE 5320. Class Lecture, Topic: “Harmonic Drive.” Dept. of Electrical and Computer Engineering, Utah State University, Logan, UT, Mar. 11, 2010.
[15] G. A. Pratt and M. Williamson, “Series Elastic Actuators.”. *Intelligent Robots and Systems 95.'Human Robot Interaction and Cooperative Robots', Proceedings. 1995 IEEE/RSJ International Conference on*. Vol. 1. IEEE, 1995.
[16] V. Chernyak, “The Design and Realization of a Sensitive Walking Platform” Worcester Poly. Inst. MA, URN etd-042412-160012. 2012
[17] G. Lazaridis, “How Brushless Motors Work (BLDC Motors),” [Online]. Available: http://pcbheaven.com/wikipages/How_Brushless_Motors_Work/.
[18] L. George, “Stepper Motor or Step Motor,” [Online]. Available: https://electrosome.com/stepper-motor/.

[19] E. Cenciper, “How to Select a Motor? (Part 2) – Understand Motor Specification,” [Online]. Available: http://www.robot-and-machines-design.com/en/Articles/Mechanics/Tips-Guides/557-Motor-Selection-How-To-Select-A-Motor-Understand-Motor-Specification.html.
[20] J. Pearman, “Motor Torque-speed Curves,” [Online]. Available: http://www.vexforum.com/showthread.php?t=70588.
[21] DraganFly, “Manual of Thunder Power Sensor less Brushless Motor Speed Controller ESC,” [Online]. Available: http://www.rctoys.com/pr/pr-html/thunder-power-brushless-speed-controller-esc-manual.htm.
[22] US Digital, “E4T OEM Miniature Optical Kit Encoder,” [Online]. Available: http://www.usdigital.com/products/encoders/incremental/rotary/kit/E4T?specification=phase-relationship.
[23] RobotShop, “ENC300CPR Easy Roller 300 CPR Quadrature Encoder.” [Online]. Available: http://www.robotshop.com/en/solutions-cubed-enc300cpr-easy-roller.html.
[24]US Digital, “MAE3 Absolute Magnetic Kit Encoder,” [Online]. Available: http://www.usdigital.com/products/encoders/absolute/rotary/kit/mae3.
[25] Digi-Key, “AEAT-6010-A06,” [Online]. Available: http://www.digikey.com/product-detail/en/AEAT-6010-A06/516-2635-ND/2210457.
[26] Sparkfun, “I2C,” [Online]. Available: https://learn.sparkfun.com/tutorials/i2c.
[27] Avago, “AEAT-6010/6012 Magnetic Encoder datasheet,” 2011.
[28] Experimentalev, “Motor Brush Replacement – A Step by Step How To,” [Online] Available: https://experimentalev.wordpress.com/2011/03/22/motor-brush-replacment-how-to/
[29] GrabCAD, “Systems engineers, the multi-domain 3D revolution is coming for you,” [Online] Available: http://blog.grabcad.com/blog/2015/03/18/multi-domain-3d-revolution/
[30] Wikipedia, “Polylactic acid,” [Online] Available: https://en.wikipedia.org/wiki/Polylactic_acid
[31] Atmel, “Atmel 8-bit microcontroller,” [Online] Available: http://www.atmel.com/Images/Atmel-8271-8-bit-AVR-Microcontroller-ATmega48A-48PA-88A-88PA-168A-168PA-328-328P_datasheet.pdf
[32] Hobbypartz, “Exceed RC Rocket 2205-1400KV Brushless Motor,” [Online] Available: http://www.hobbypartz.com/86ma01-2205-1400kv.html
[33] Hobbyking, “Turnigy TrackStar 25A Brushless ESC,” [Online] Available: http://www.hobbyking.com/hobbyking/store/__14630__Turnigy_TrackStar_25A_1_18th_Scale_Brushless_Car_ESC.html